Spectrochimica Acta, Vol. 40A, No. 6, pp. 481–501, 1984
Printed in Great Britain.

0584–8539/84 $3.00 + 0.00

Vibrational analysis of crystalline diketopiperazine—I. Raman and i.r. spectra*

T. C. CHEAM and S. KRIMM

Department of Physics and Biophysics Research Division, University of Michigan, Ann Arbor, MI 48109, U.S.A.

(*Received* 29 *November* 1983)

Abstract—Raman and i.r. spectra have been obtained of diketopiperazine and five of its isotopic derivatives: $(CONDCH_2)_2$, $(CONHCD_2)_2$, $(CONDCD_2)_2$, $(^{13}CONHCH_2)_2$ and $(^{13}CONDCH_2)_2$. In addition to solution spectra and powder spectra at room and liquid nitrogen temperatures, polarized Raman spectra were obtained on single crystals. These data have permitted an essentially complete assignment to be made of the Raman and i.r. modes of the crystal, a necessary step in the refinement of an intramolecular force field for this molecule [13].

INTRODUCTION

Diketopiperazine (DKP), $(CONHCH_2)_2$, is a simple model compound that is useful in studying the vibrational modes of the *cis* peptide group. Infrared (i.r.) spectra of DKP and its *N*-deuterated derivative (NdDKP) have been obtained by several authors [1–6], and the Raman spectrum of DKP has been reported [7]. An extensive set of i.r. and Raman data on DKP, NdDKP and the *C*-deuterated compounds (CdDKP and NCdDKP) was obtained by STEIN [8]. Normal mode calculations have also been done [6, 8–10].

Despite the large amount of work on DKP, some important aspects of the analysis are not yet satisfactory. In the i.r., the assignments of two peptide group vibrations, NH in-plane bend (ib) and CN stretch (str), and the CH_2 bend mode are not unequivocal because only two bands have been observed in the 1400–1500 cm^{-1} region; various schemes of overlap have had to be assumed [4, 6, 8]. The CO out-of-plane bend (ob) has either been left unassigned [8, 9] or was thought to be overlapped with CO ib [6]. Each normal mode calculation has used an approximate structural model instead of the exact X-ray structure of DEGEILH and MARSH [11]; moreover, FUKUSHIMA *et al.* [9] and STEIN [8] took the CH_2 groups to be point masses. All previous workers considered an isolated molecule in their calculations, except for STEIN who took into account in parts of his analysis the hydrogen bonds between translationally equivalent molecules in a chain. The force fields used were of the Urey–Bradley type, and only ASAI *et al.* [6] attempted a systematic refinement of the force constants; these authors, however, did not use any Raman data, and there are significant discrepancies between calculated and observed frequencies for several i.r. modes.

Our aim in these papers is to present a more comprehensive experimental and theoretical vibrational analysis of DKP in the crystalline state. This is part of a program of applying vibrational spectroscopy to the study of structure in peptides, polypeptides and proteins [12]. In addition to helping to elucidate the normal modes of the *cis* peptide group, this study is important because DKP is the simplest cyclic peptide. Furthermore, DKP is a peptide crystal of relatively high symmetry and simplicity (the asymmetric unit is just one $CONHCH_2$ group), thus making it a convenient system for studying intermolecular interactions in peptides and polypeptides.

In the present paper, we describe our Raman and i.r. experimental data and their analysis. Paper II [13] deals with the normal coordinate calculations, including the refinement of an intramolecular valence force field for DKP.

EXPERIMENTAL

DKP was synthesized from glycine using procedures described by GREENSTEIN and WINITZ [14]. The *N*-deuterated compound, $(CONDCH_2)_2$, was obtained from D_2O solution. Four other isotopic derivatives, $(CONHCD_2)_2$, $(CONDCD_2)_2$, $(^{13}CONHCH_2)_2$ and $(^{13}CONDCH_2)_2$, were also prepared starting with glycine-d_5 (98% purity, Aldrich) and with $H_2NCH_2{}^{13}COOH$ (90% atom ^{13}C, Merck). The *C*-deuterated materials were also obtained by refluxing DKP in D_2O [8], but the degree of isotopic substitution was poor.

Single crystals, measuring a few mm on a side, of all the compounds except $(^{13}CONDCH_2)_2$ were grown from aqueous solution by slow evaporation at 50–70°C. Single crystal films for polarized i.r. studies were prepared by cleaving from thicker pieces. The DKP unit cell is monoclinic with space group C_{2h}^5 [11] (see Fig. 1). We determined the orientation of the crystal axes in each of our specimens and checked for twinning by optical examination and cleavage [15, 16].

Our i.r. spectra were run on a Perkin–Elmer 180 spectrophotometer; the bandpass was about 2 cm^{-1} in the 400–2000 cm^{-1} region. The Raman spectrometer used was based on a Spex 1400 double monochromator equipped with holographic gratings [17]. We used the 514.5 nm line of a Coherent Radiation 52 argon ion laser; typical instrumental settings for our solid state spectra were 0.3 cm^{-1} bandpass and 500 mW laser power. Spectra were obtained at room

*This is paper number 22 in a series, "Vibrational analysis of peptides, polypeptides and proteins", of which [12] is paper number 21.

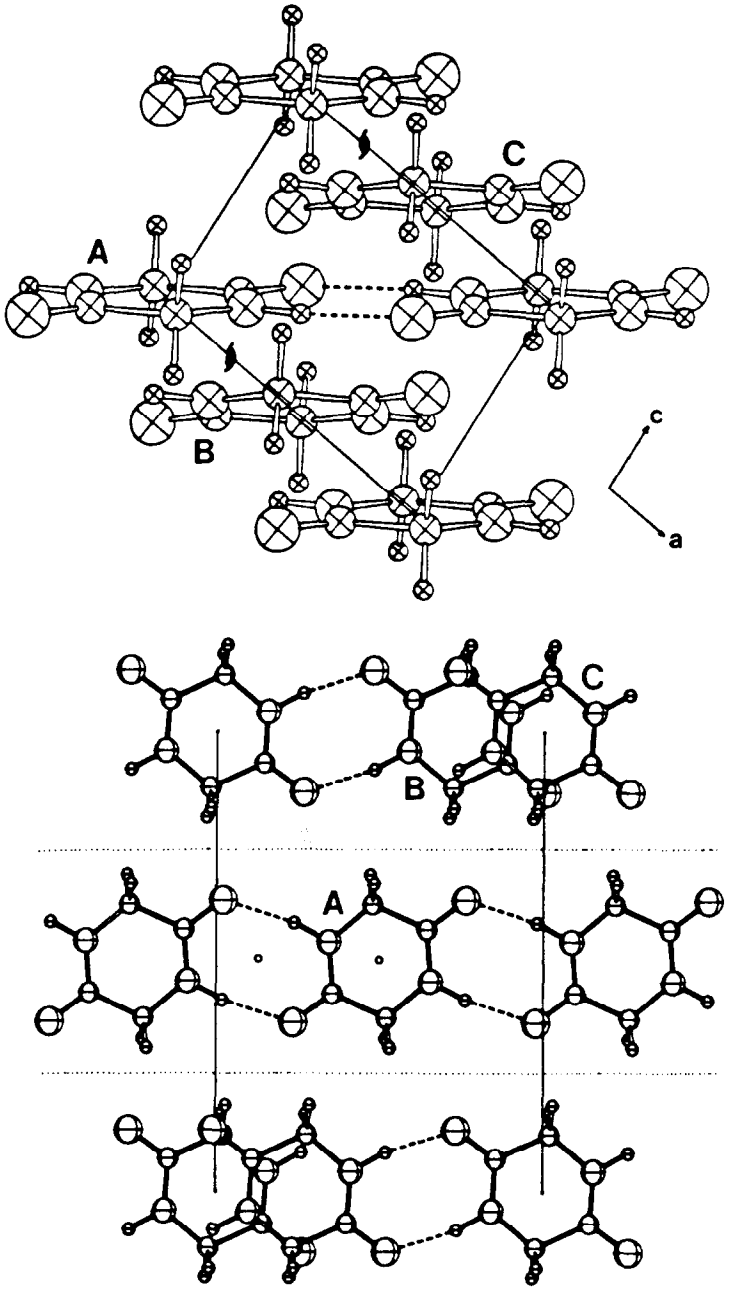

Fig. 1. Diketopiperazine crystal. Top: viewed along b axis. Bottom: viewed perpendicular to $(10\bar{1})$. Molecules are related to each other by a twofold screw axis, $C_2^5(b)$, at $a_0/4$ and a glide plane $\sigma_h^a(ac)$, at $b_0/4$ with translation $a_0/2$.

temperature (RT) and at liquid nitrogen temperature (LT), the latter with home-made cryostats. Infrared spectra of polycrystalline powdered samples were run in KBr pellets. For the Raman spectra the powder was pressed into free-standing films. Solution spectra were obtained using standard i.r. liquid cells and, for the Raman measurements, glass capillaries; to increase the solubility of the samples the solutions were kept at elevated temperatures using heating tape around the cells or capillaries. For the single crystal Raman experiments we used a 90° scattering geometry. Since the DKP crystal has an inversion center, it is not optically active. To avoid birefringence effects [18], we chose as polarization directions [101], b and $\perp$ $(10\bar{1})$ because the two symmetry-unrestricted principal axes of the indicatrix are approximately along [101] and perpendicular to (101) [15, 16]. The directions [101], b and $\perp$ $(10\bar{1})$ are denoted as X, Y and Z, respectively. Five elements of the Raman tensor were examined: XX, ZZ, XY, XZ and ZY. The sixth element, YY, was not measured because of a low degree of polarization caused by poorly formed faces in the $X(YY)Z$ orientation.

SPECTRAL ASSIGNMENTS

Our Raman and i.r. spectra are shown in Figs. 2–17. Figure 18 shows the far i.r. spectra of DKP at RT and

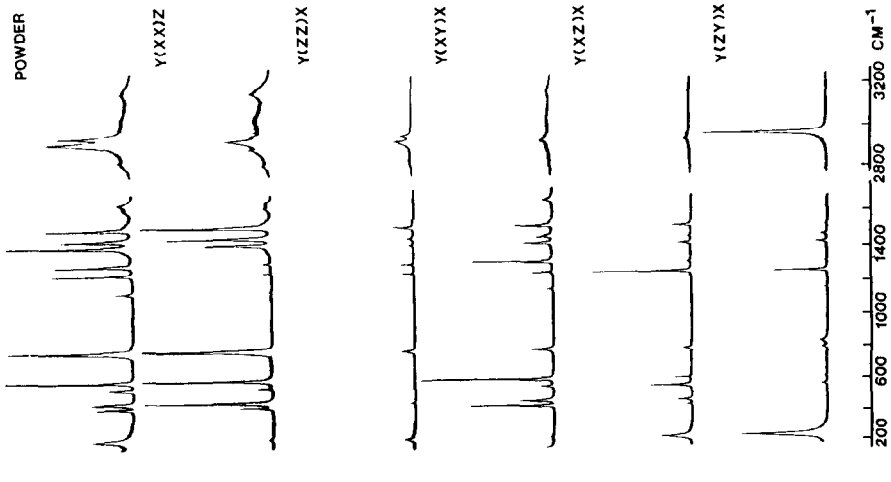

Fig. 2. Raman spectra of DKP powder and single crystal.

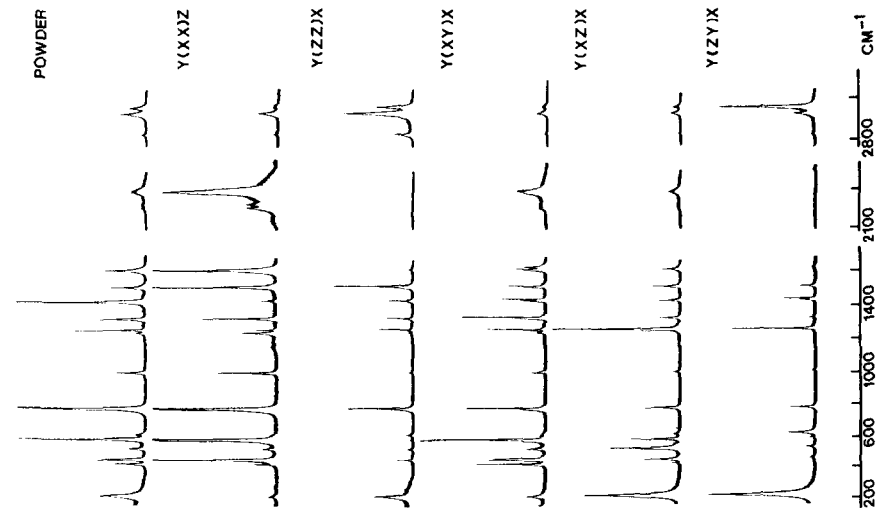

Fig. 3. Raman spectra of NdDKP powder and single crystal.

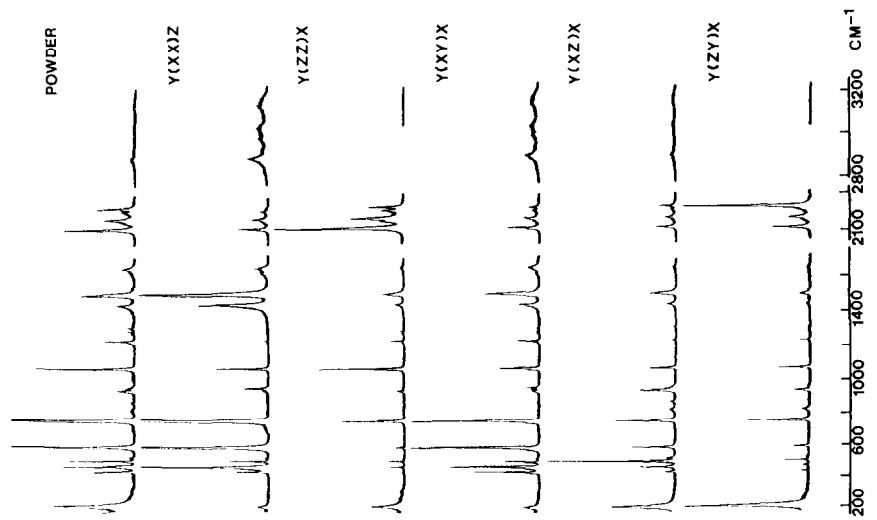

Fig. 4. Raman spectra of CdDKP powder and single crystal.

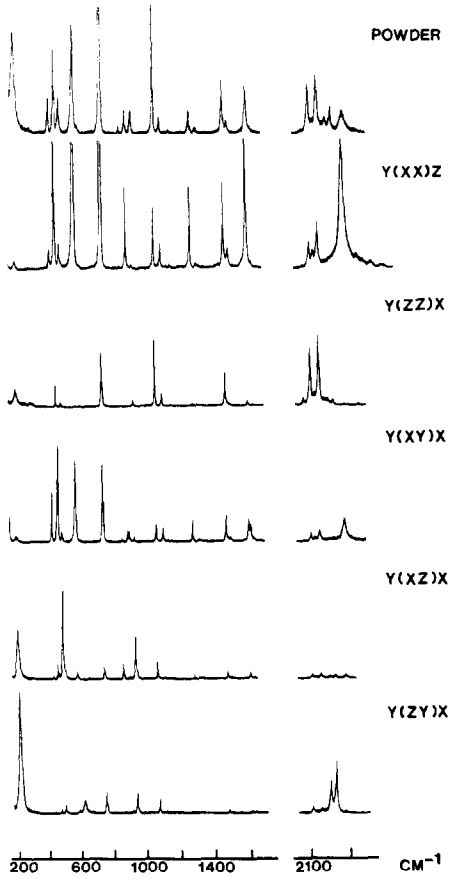

Fig. 5. Raman spectra of NCdDKP powder and single crystal.

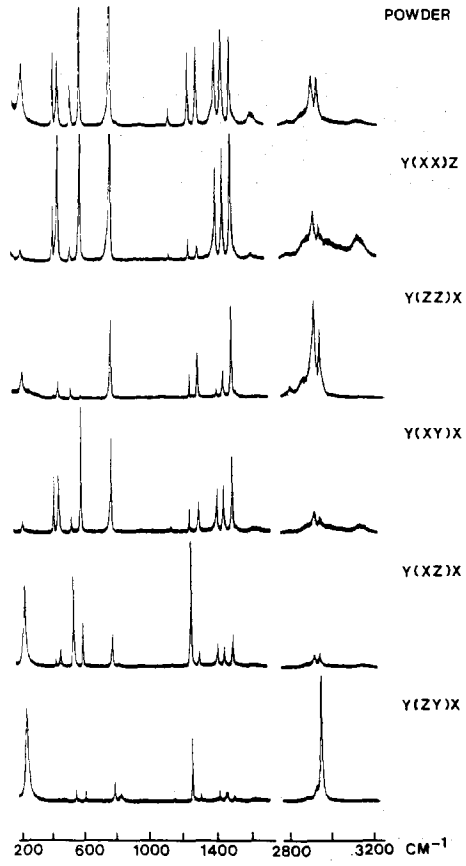

Fig. 6. Raman spectra of C13DKP powder and single crystal.

LT, obtained on an IBM Fourier transform instrument by Dr. JOHN F. RABOLT. Because there are no qualitative differences in the low frequency Raman spectra ($< 200\,cm^{-1}$) of the various isotopic compounds, we give the powder and single crystal spectra of only DKP in this region. In the high frequency i.r. spectra bands due to atmospheric CO_2 at about $2360\,cm^{-1}$ are represented by dotted segments when these were prominent. The broad band near $3450\,cm^{-1}$ is due to absorption by residual H_2O in the KBr powder.

According to the study of DEGEILH and

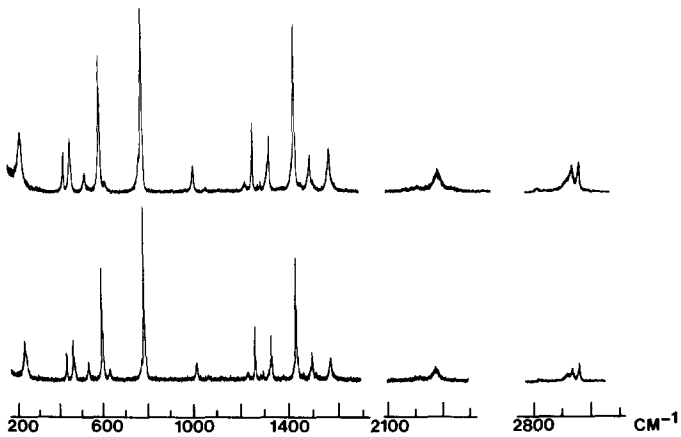

Fig. 7. Raman spectra of NdC13DKP powder. Top: RT. Bottom: LT.

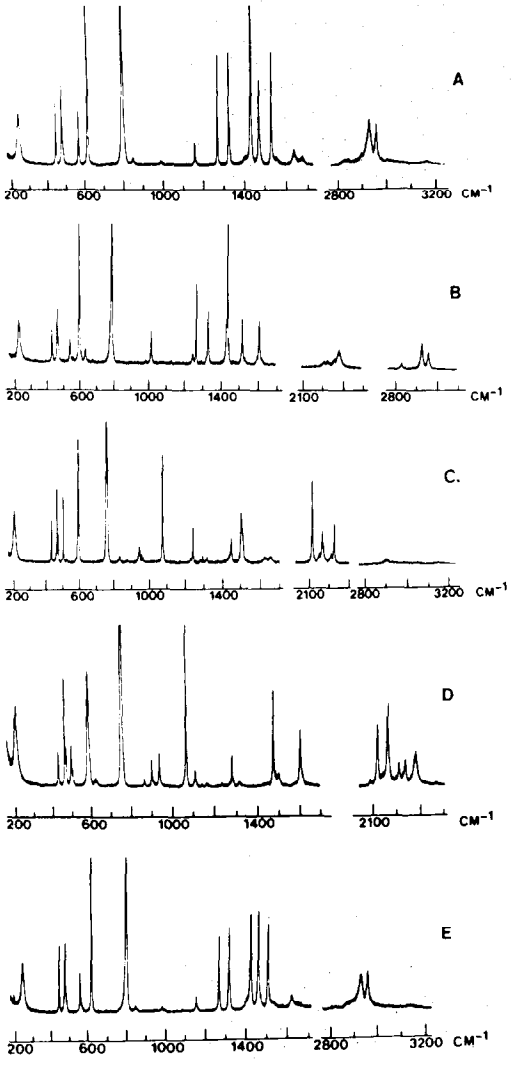

Fig. 8. LT Raman spectra of powder samples. A–E: DKP, NdDKP, CdDKP, NCdDKP, C13DKP.

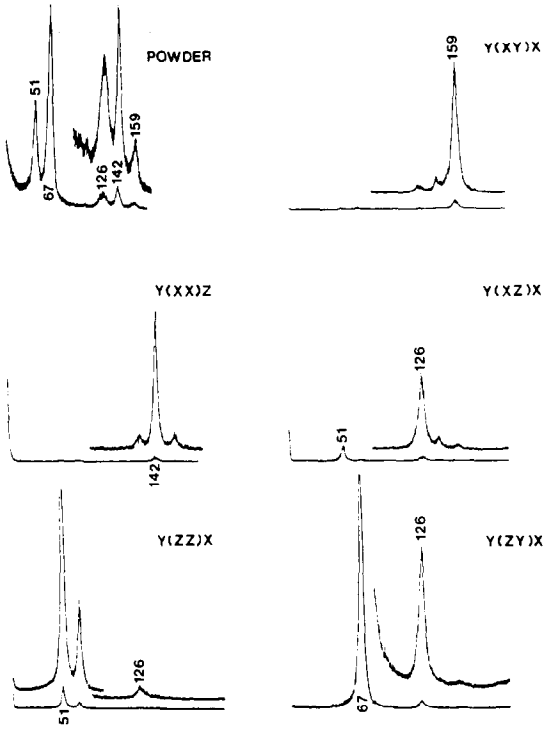

Fig. 9. Low frequency Raman spectra of DKP.

MARSH [11], the DKP molecule belongs to the point group C_i. The 36 vibrational modes of a molecule are therefore classified as $18\,a_g + 18\,a_u$. Though the heavy atoms are essentially coplanar [11, 19], the angles about the CH_2 groups show that the hydrogen atoms are not symmetrically located. Thus, there is no plane of symmetry in the DKP molecule. However, if one assumes such a plane of symmetry, as other workers have done, one can further classify the internal modes

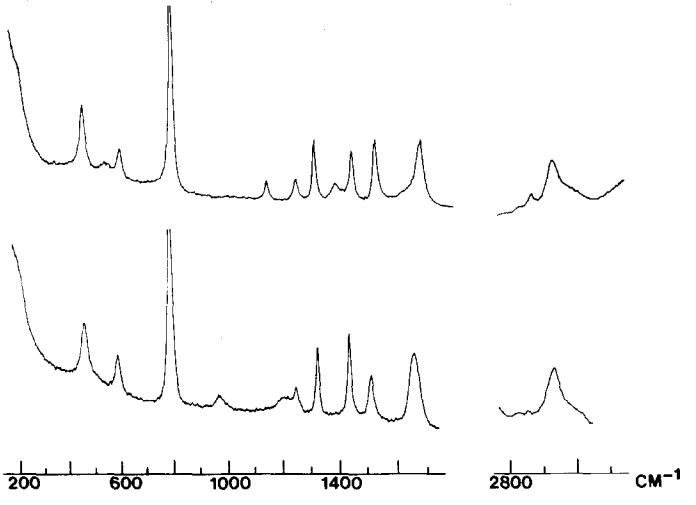

Fig. 10. Raman spectra of DKP in solution at 70°C. Top: H_2O. Bottom: D_2O.

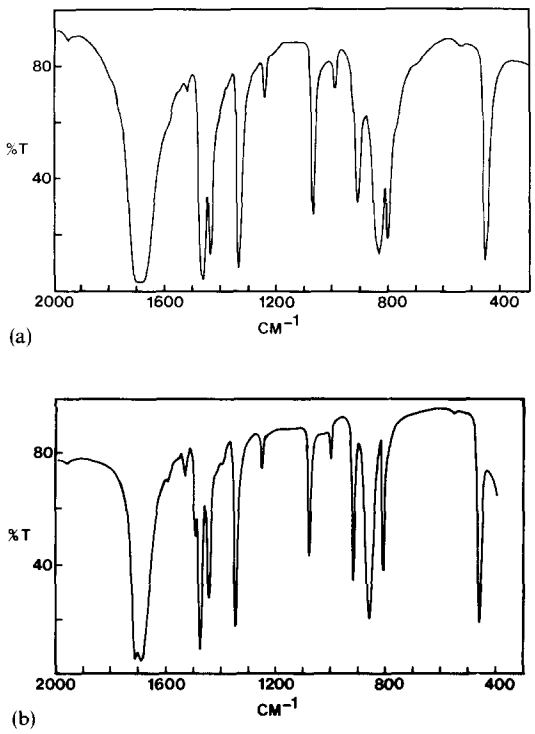

Fig. 11. Infrared spectra of DKP powder. (a) RT, (b) LT.

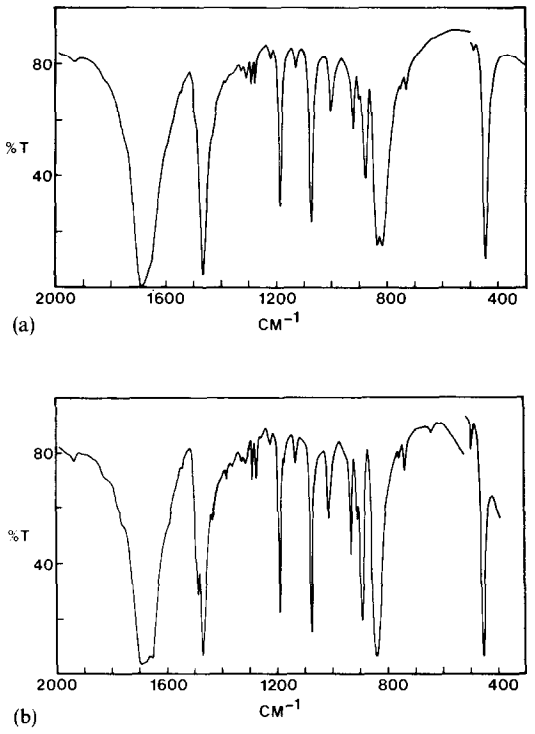

Fig. 13. Infrared spectra of CdDKP powder. (a) RT, (b) LT.

into in-plane or out-of-plane vibrations. The Raman active modes of such a C_{2h} model are then described as 12 in-plane (a_g of C_{2h}) and six out-of-plane (b_g), and the i.r. active modes are 11 in-plane (b_u) and seven out-of-plane (a_u of C_{2h}). In the crystal, with two molecules in a unit cell, each internal mode splits into two, an A_g–B_g or A_u–B_u pair.

Our single crystal Raman spectra may be analysed to

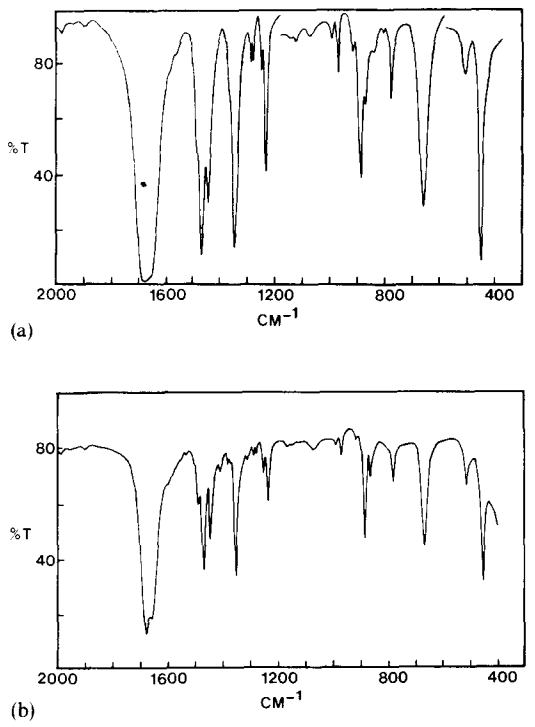

Fig. 12. Infrared spectra of NdDKP powder. (a) RT, (b) LT.

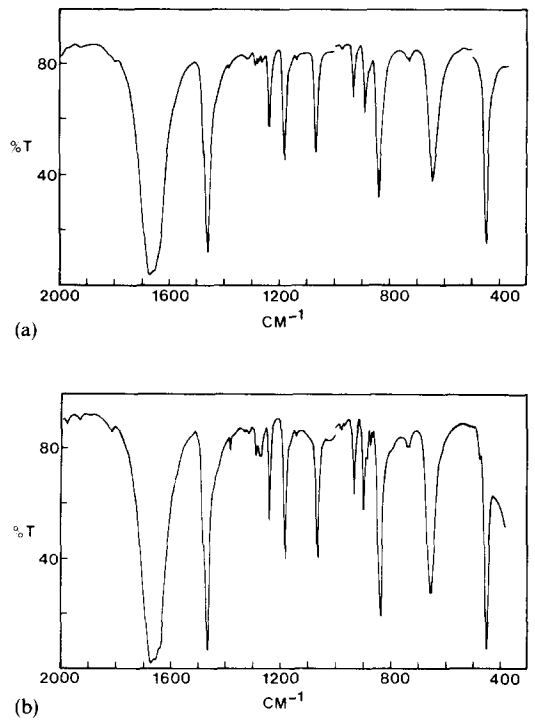

Fig. 14. Infrared spectra of NCdDKP powder. (a) RT, (b) LT.

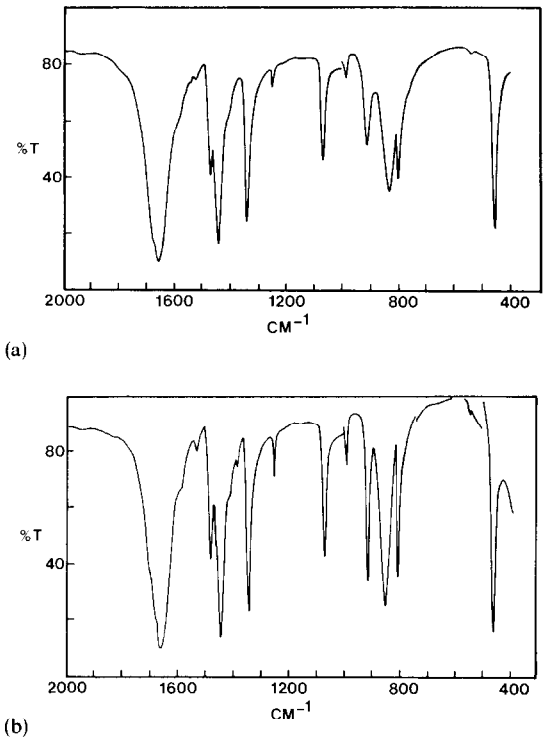

Fig. 15. Infrared spectra of C13DKP powder. (a) RT, (b) LT.

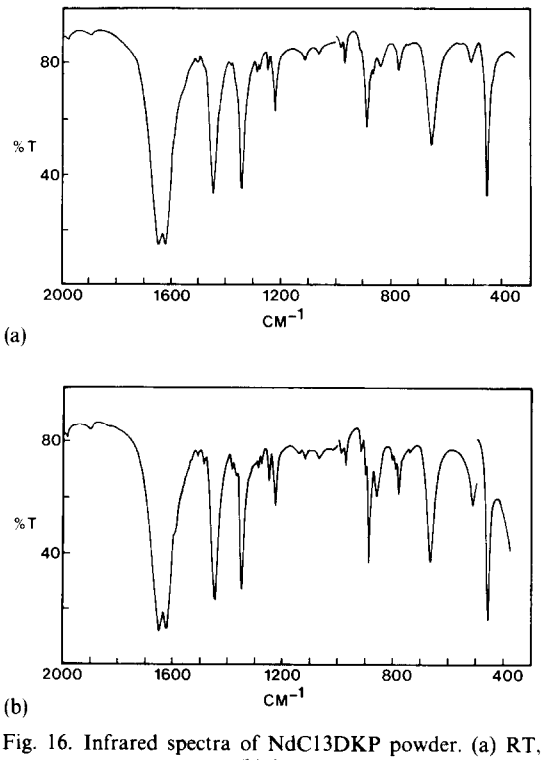

Fig. 16. Infrared spectra of NdC13DKP powder. (a) RT, (b) LT.

yield the symmetry species of the internal modes according to either the exact C_{2h}^5 space symmetry or the approximate C_{2h} point symmetry. The lattice modes are, of course, best described by the space group species. Thus, bands of A_g symmetry appear in the XX, ZZ and XZ spectra, while B_g bands appear in the XY and ZY spectra. The plane of symmetry of a C_{2h} molecular model is inclined at about 9° to the $(10\bar{1})$ or XY plane [20]. It is possible to transform the molecular tensor to the crystal axes and to obtain the precise relationships between the molecular and crystal tensor elements in the oriented gas approximation [21]. However, the transformation matrix in our case is so close to the identity that we may take the two sets of axes to be coincident. We then conclude that bands that are strong in the XX, ZZ and XY spectra are due to in-plane (a_g) vibrations, while the out-of-plane (b_g) modes appear strong in the XZ and ZY polarizations. Though we do not have $YY(A_g/a_g)$ spectra, the relative intensity of a mode in this polarization may be estimated by comparing its intensity in the powder spectra with that observed in the five polarizations actually measured.

Tables 1–4 list the observed frequencies and their assignments. By comparison with spectra of less completely deuterated samples, we eliminated many bands as being due to impurities. We agree with ASAI *et al.* [6] that the i.r. bands found near 1280 and 1290 cm^{-1} in NdDKP are CHD absorptions. These bands are also present in other deuterated samples and in the Raman spectra as well, and are especially strong in partially *C*-deuterated materials prepared by refluxing DKP in D_2O. Furthermore, preliminary calculations with CHD groups in DKP (D atoms placed such that the inversion symmetry is preserved) predict CHD vibrations (bend and wag) in this region, regardless of whether NH or ND is also present.

We now proceed to discuss our assignments. The important mid-frequency region (200–1700 cm^{-1} in Raman, and 400–1800 cm^{-1} in i.r.) will be considered first, followed by the high frequency region and then the low frequency region. In our analysis we have made use of information such as polarization data, isotope shift, intensity, temperature behavior and, in a few cases, calculations. The characterization of the modes can only be approximate at this stage; more precise descriptions can only be gained from a satisfactorily refined force field. We will not refer to modes as amide I, II, etc. since these names refer to modes that are well characterized at present only for *trans* peptide groups. Their use for *cis* peptide vibrations can be confusing because of differences in the nature of the modes. In addition, the modes of *cis* peptides are not yet well understood for a sufficiently large set of compounds to be classified as characteristic group vibrations.

Raman in mid-frequency region

All Raman active fundamentals in this region are, we feel, definitively assigned for all six isotopic species. Our assignments for DKP and NdDKP agree with STEIN's [8] except for the 1391 cm^{-1} band in DKP, which we do not think is a fundamental. (Note that

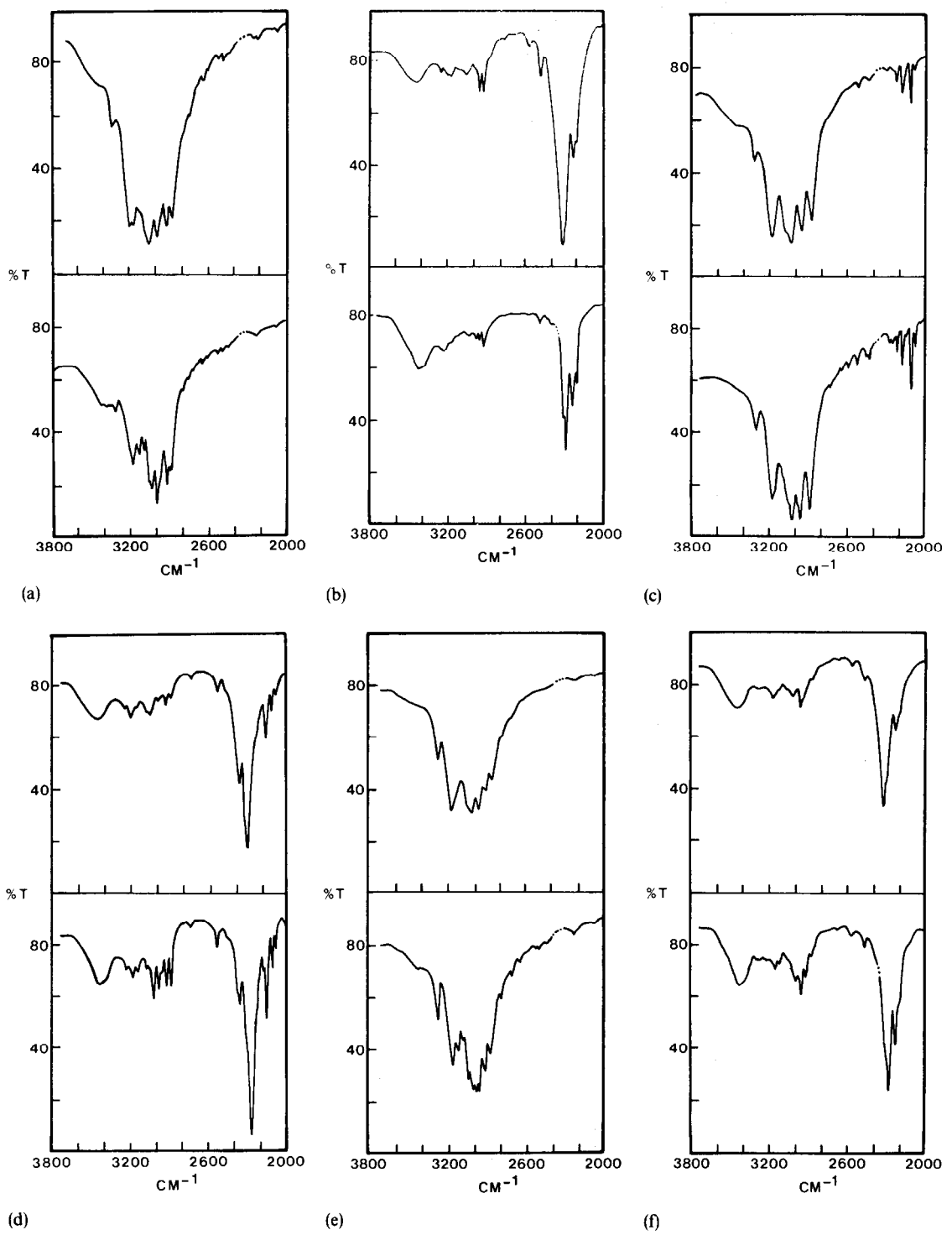

Fig. 17. High frequency i.r. powder spectra of (a) DKP, (b) NdDKP, (c) CdDKP, (d) NCdDKP, (e) C13DKP, (f) NdC13DKP. Top: RT. Bottom: LT.

STEIN preferred the "amide mode" nomenclature.)

Vibrations of CONH group. The highest frequency band in this region is clearly the CO str mode. It shows some very interesting features and behavior. Its appearance is simplest in the *N*-deuterated materials and in solution. In the latter case it is broad, is one of the strongest bands and shows a shift of 19 cm^{-1} from H_2O to D_2O solution. There is an even larger drop ($\sim 50\,cm^{-1}$) from D_2O solution to crystalline NdDKP, and ^{13}C-substitution of NdDKP causes an

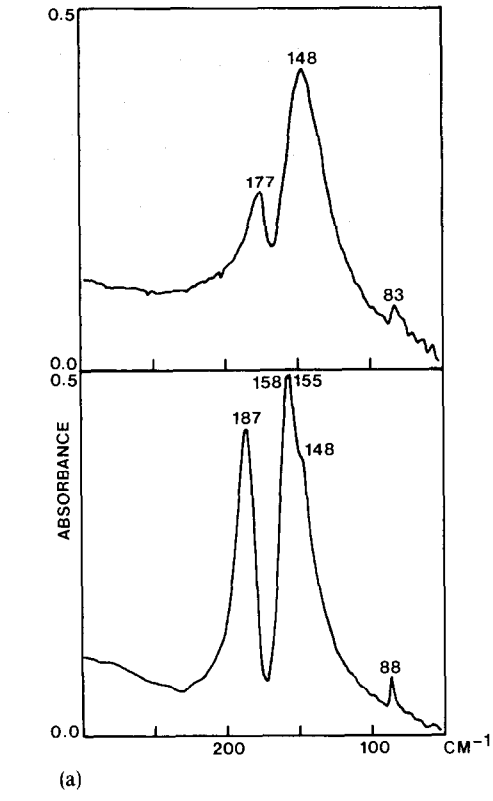

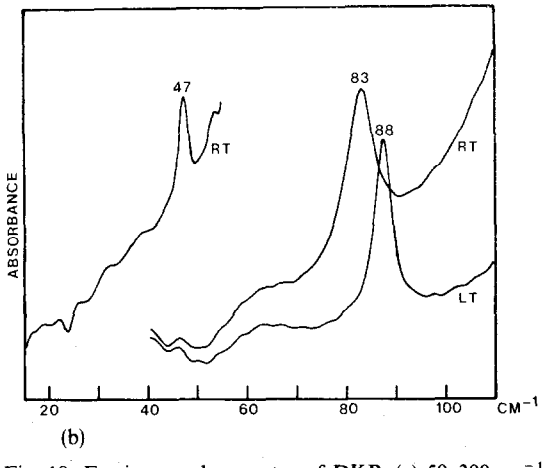

Fig. 18. Far i.r. powder spectra of DKP. (a) 50–300 cm^{-1} region. Top: RT. Bottom: LT. (b) 20—100 cm^{-1} region.

Table 1. Raman frequencies (in cm^{-1}) of crystalline diketopiperazine*

LT	RT	Symm.	Assign.
$(CONHCH_2)_2$			
3158	3160 vw	a_g	· NH str
3101	3106 vvw		
	3035 vw	a_g	
2996 vw			
2958	2954 m	b_g	CH_2 as
2927	2929 m	a_g	CH_2 ss
2896	2899 sh		
2832	2835 w	a_g	

Table 1. (continued)

LT	RT	Symm.	Assign
	1664 vw	a_g B_g	CO str
1666	1652 w	a_g A_g	
1626	1623 w	a_g A_g	
1547	1549 vw		
1519	1519 m	a_g	Ring str
1462	1457 m	a_g	NH ib
1423	1422 vs	a_g	CH_2 b
1393	1391 vw		
1322	1319 w	a_g B_g	CH_2 wag
1318	1313 m	a_g A_g	
1264	1261 m	b_g	CH_2 t
	1155 vw	B_g	NC^{α} str
1152	1149 w	a_g A_g	
983	985 vw		CH_2 r
844	832 vw	b_g	NH ob
793	795 vs	a_g	Ring str
613	612 vs	a_g	CO ib
563	561 m	b_g	CO ob
482	480 w	a_g B_g	Ring ib
476	473 m	a_g A_g	
443	443 m	a_g	Ring ib
	342 vw		
242	236 m	b_g	Ring tor
166	159 m	B_g	Lattice
147	142 s	A_g	Lattice
130	126 s	A_g B_g	Lattice
71	67 vvs	B_g	Lattice
54	51 vs	A_g	Lattice
$(CONDCH_2)_2$			
2954	2954 m	b_g	CH_2 as
2923	2934 m	a_g	CH_2 ss
	2883 vvw		
2828	2826 w	a_g	
2279	2290 m	a_g	
2259 sh			
2226	2220 w	a_g	ND str
2206	2202 w	a_g	
1614	1617 vw	a_g B_g	CO str
1599	1602 m	a_g A_g	
1587	1589 sh		
1522	1520 sh		Impurity
1510	1508 m	a_g	Ring str
1464	1461 vvw		Impurity
1437	1436 vw	B_g	CH_2 b
1430	1429 vs	a_g A_g	
1379	1374 vvw		
1331	1328 vw	a_g B_g	CH_2 wag
1328	1323 m	a_g A_g	
1319	1315 sh		Impurity
1291	1291 vw		Impurity
1280	1280 vw		Impurity
1262	1259 m	b_g	CH_2 t
1243	1241 w	a_g	NC^{α} str, ND ib
1124	1122 vvw		Impurity
1060	1062 vvw		Impurity
	1015 vw	B_g	NC^{α} str, ND ib
1013	1008 m	a_g A_g	
981	982 vvw		CH_2 r
787	787 vs	a_g	Ring str
634	626 w	b_g	ND ob
609 vw			
598	596 vs	a_g	CO ib
561	558 vw		Impurity
544	537 w	b_g	CO ob
477	474 w	B_g	Ring ib
470	469 m	a_g A_g	
437	437 m	a_g	Ring ib
	289 vvw		

Table 1. (continued)

LT	RT	Symm.	Assign.
240	232 m	b_g	Ring tor
163	157 m	B_g	Lattice
146	140 s	A_g	Lattice
127	123 s	A_g B_g	Lattice
70	67 vvs	B_g	Lattice
54	51 vs	A_g	Lattice
$(CONHCD_2)_2$			
3145	3151 vvw		NH str
3031	3040 vvw		
2994	2992 vvw		
2941	2934 vw		
2899	2896 vw	a_g	
2378	2376 vvw		
2222	2222 m	b_g	CD_2 as
2208	2202 w	a_g	CD_2 ss
2163	2163 m	a_g	
2146 w	2148 sh		
2113	2114 m	a_g	
	1652 vw	B_g	CO str
1651	1645 w	a_g A_g	
1620 w	1613 sh	A_g	
1499	1496 m	a_g	Ring str
1445	1437 m	a_g	NH ib
1313	1311 vw		Impurity
1289	1289 vw		Impurity
1277	1278 vw		Impurity
1239	1235 m	a_g	NC^a str, CD_2 wag
1222	1221 vw		Impurity
1076	1076 w	B_g	CD_2 b
1070	1071 s	a_g A_g	
962	962 vw	B_g	CD_2 wag
952	953 vw	$a_g A_g$	
942	941 w	b_g	CD_2 t
939 sh			
875	870 vw	b_g	CD_2 r
830 w	823 vw	b_g	NH ob
762	763 m		Impurity
757	757 vs	a_g	Ring str
594	590 s	a_g	CO ib
525	523 vw		Impurity
506	504 m	b_g	CO ob
475	475 w	B_g	Ring ib
469	468 m	a_g A_g	
434	434 m	a_g	Ring ib
213	208 m	b_g	Ring tor
161	155 m	B_g	Lattice
143	138 s	A_g	Lattice
127	123 s	A_g B_g	Lattice
69	66 vvs	B_g	Lattice
52	49 vs	A_g	Lattice
$(CONDCD_2)_2$			
2364	2359 vvw		
2275	2290 m	a_g	ND str
2232	2230 w	b_g	CD_2 as
2205	2201 w	b_g	
2157	2157 m	a_g	CD_2 ss
2133	2132 vvw		
2112	2112 m	a_g	CD_2 ss
2080	2075 vvw		
1610 sh	1613 vw	B_g	CO str
1600	1602 m	a_g A_g	
1502	1498 w		Impurity
1487	1482 sh		Impurity
1476	1472 m	a_g	Ring str
1319	1320 vw		Impurity
1294	1295 vw		Impurity
1287	1284 w	a_g	NC^a str, ND ib
1168	1165 vvw		Impurity

Table 1. (continued)

LT	RT	Symm.	Assign
1146	1145 vvw		Impurity
1114	1110 w	a_g	NC^a str, ND ib
	1075 w	B_g	CD_2 b
1070	1070 s	a_g A_g	
941	940 w	b_g	CD_2 t
913	913 vw	B_g	CD_2 wag
905	902 w	a_g A_g	
866	867 vw	b_g	CD_2 r
757	754 m		Impurity
751	750 vs	a_g	Ring str
621	616 vw	b_g	ND ob
586	585 m	a_g	CO ib
506	502 sh		Impurity
499	495 w	b_g	CO ob
474	473 w	a_g B_g	Ring ib
467	464 m	a_g A_g	
430	432 w	a_g	Ring ib
211	205 m	b_g	Ring tor
160	153 m	B_g	Lattice
143	136 s	A_g	Lattice
126	121 s	A_g B_g	Lattice
69	64 vvs	B_g	Lattice
53	49 vs	A_g	Lattice
$(^{13}CONHCH_2)_2$			
3133	3139 vw	a_g	NH str
	3057 vvw		
	3003 vvw		
2954	2955 m	b_g	CH_2 as
2927	2929 m	a_g	CH_2 ss
2874	2873 sh		
2816	2813 vw		
1651 vw	1632 sh		CO str
1614	1615 w	a_g A_g	
1521	1522 sh		
1499	1501 m	a_g	Ring str
1452	1451 m	a_g	NH ib
1416	1412 m	a_g	CH_2 b
1396	1396 sh		
1314	1311 w	B_g	CH_2 wag
1310	1308 m	a_g A_g	
1261	1259 m	b_g	CH_2 t
1157	1154 sh	B_g	NC^a str
1148	1145 w	a_g A_g	
975	977 vw		CH_2 r
843	831 vw	b_g	NH ob
794	795 vs	a_g	Ring str
612	611 vs	a_g	CO ib
551	549 m	b_g	CO ob
477 sh			Ring ib
470	471 m	a_g A_g	
440	441 m	a_g	Ring ib
241	236 m	b_g	Ring tor
163	159 m	B_g	Lattice
146	141 s	A_g	Lattice
128	125 s	A_g B_g	Lattice
70	67 vvs	B_g	Lattice
54	51 vs	A_g	Lattice
$(^{13}CONDCH_2)_2$			
2955	2953 m		CH_2 as
2931	2929 m		CH_2 ss
2915 w	2915 sh		
2816	2812 vw		
2275	2286 m		ND str
2217	2215 vvw		
2197	2197 vvw		
2167	2167 vvw		
1565	1567 m		CO str (A_g)
1506	1504 vw		

Table 1. (continued)

LT	RT	Symm.	Assign.
1490	1489 m		Ring str
1484	1483 sh		
1434 sh			CH_2 b
1427	1426 s		
1328	1325 sh		CH_2 wag
1325	1321 m		
1320 w	1307 sh		Impurity
1290	1290 vw		Impurity
1281	1279 vw		Impurity
1259	1256 m		CH_2 t
1228	1225 w		NC^{α} str, ND ib
1119	1116 vvw		Impurity
1061	1058 vvw		Impurity
1010	1007 m		NC^{α} str, ND ib
978	977 vvw		CH_2 r
785	785 vs		Ring str
771 w	774 sh		Impurity?
629	620 w		ND ob
602 w	598 sh		Impurity?
596	594 s		CO ib
551	547 vvw		Impurity
531	528 w		CO ob
472	470 sh		Ring ib
465	464 m		
433	433 m		Ring ib
238	232 m		Ring tor
160	155 m		Lattice
143	138 s		Lattice
127	122 s		Lattice
68	64 vvs		Lattice
53	49 vs		Lattice

*Abbreviations; LT = low temperature; RT = room temperature; s = strong; m = medium; w = weak; v = very; sh = shoulder; str = stretch; as = antisym. str; ss = sym. str; b = bend; r = rock; t = twist; ib = in-plane bend; ob = out-of-plane bend; tor = torsion.

Table 2. Infrared frequencies (in cm^{-1}) of crystalline diketopiperazine*

LT	RT	Assign.
$(CONHCH_2)_2$		
3312	3325 vw	
3200 sh		
3180	3192 w	
3135	3165 w	
3095 w	3113 vw	
3054 w	3077 sh	
3035	3046 w	
2996 m	2986 w	Mainly NH str
2973 sh		
2954	2954 sh	
2936 sh		
2921 m	2915 w	
2900 w		
2884	2875 w	
2860 sh		
1712 vs	1697 vs	
1692 sh		CO str
1682 vs	1678 sh	
1530	1525 vw	
1493 w	1482 sh	NH ib
1479 sh		

Table 2. (continued)

LT	RT	Assign.
1475	1470 s	Ring str
1459 vvw	1458 sh	
1446	1445 m	CH_2 b
1438	1438 sh	
1348 s	1343 s	CH_2 wag
1345 s		
1254	1252 w	CH_2 t
1080	1075 m	NC^{α} str
996	993 w	CH_2 r
914	913 m	Ring ib, ring str
856	837 s	NH ob
809	805 m	Ring ib, ring str
565 sh		
553	553 vvw	CO ob
451	447 s	CO ib
187 m	177 w	Ring tor
158 m		
155 m	148 m	Lattice
148 sh		
88	83 vw	Lattice
	63 vvw	
	47 vvw	Lattice
$(CONDCH_2)_2$		
2954	2952 w	CH_2 as
2921	2922 w	CH_2 ss
2491	2483 w	
2403 vvw	2400 sh	
2312 w	2319 s	
2294 s	2298 sh	ND str
2246 m	2236 w	
2228 sh		
2212	2207 w	
1682	1681 vs	CO str
1659 s	1655 sh	
1505 vvw	1505 sh	
1491 w	1489 sh	
1472	1469 s	Ring str
1459	1458 sh	
1448	1447 m	CH_2 b
1440	1438 sh	
1357	1351 s	CH_2 wag
1292	1292 w	Impurity
1282	1282 w	Impurity
1255	1253 w	CH_2 t
1238	1235 m	NC^{α} str, ND ib
1127	1122 vw	Impurity
1078	1075 vw	Impurity
995	990 vw	CH_2 r
971	969 w	NC^{α} str, ND ib
922	917 vw	Impurity
887	888 m	Ring ib
	870 w	Impurity
784 m	778 w	Ring str
670	661 s	ND ob
518	510 w	CO ob
448	444 s	CO ib
$(CONHCD_2)_2$		
3300	3306 w	
3175	3175 m	
3156 sh		
3046	3070 sh	
3024	3034 m	NH str
2980 sh		
2960	2950 m	
2896 m		
2886	2875 m	
2864 sh		

Table 2. (continued)

LT	RT	Assign.
2221 w	2220 vw	CD_2 as
2178 w	2176 vw	
2150 vvw		CD_2 ss
2112 m	2110 w	
2083 vw	2078 vvw	
1692	1693 vs	
1682 vs	1677 sh	CO str
1657 s	1656 sh	
1506 sh		
1496 w	1493 vw	
1488 m	1479 vw	NH ib
	1472 sh	
1472	1466 s	Ring str
1459	1459 sh	
1454	1453 sh	
1436 vw		
1311 vw	1308 vvw	Impurity
1291 w	1291 vw	Impurity
1278 w	1278 vw	Impurity
1226 vw	1220 vvw	Impurity
1192	1189 s	CD_2 wag
1133 w	1135 vw	Impurity
1080 sh		
1077	1077 s	CD_2 b
1012 m	1005 w	NC^{α} str
1006 sh		
931 m	930 w	CD_2 t
910 w	905 sh	Impurity
893 s	885 m	CD_2 r?
843	843 m	Ring ib?
837	827 s	NH ob
743	742 vvw	Impurity
739 w	737 vw	Ring str
488 w	485 vw	CO ob
445	440 s	CO ib
$(CONDCD_2)_2$		
2529	2521 vw	
2380	2360 w	
2312	2318 sh	ND str
2278	2296 s	
2230 sh	2228 vvw	CD_2 as
2182 vw		
2156	2154 w	
2112	2110 vw	CD_2 ss
2085	2080 vw	
1677	1675 vs	
1660 vs	1658 sh	CO str
1645 s	1639 sh	
1505 vvw		
1485 sh		
1468	1462 s	Ring str
1318	1315 vvw	Impurity
1292 w	1291 vw	Impurity
1283 vw	1283 vvw	Impurity
1272 w	1268 vvw	Impurity
1243	1238 m	NC^{α} str, ND ib
1189 sh		Impurity
1184	1182 m	CD_2 wag
1170 vw	1161 vvw	Impurity
1145	1142 vw	Impurity
1069 m	1067 m	CD_2 b
1065 m		
978	973 vw	
931	930 m	CD_2 t
917 vw		Impurity
896	890 m	NC^{α} str, ND ib?
873 w	872 vw	CD_2 r?
866 vw		Impurity

Table 2. (continued)

LT	RT	Assign.
843 sh		Impurity
836	838 s	Ring ib?
745	740 vw	Impurity
732	729 vw	Ring str
657	645 s	ND ob
466	460 vw	CO ob
442	438 s	CO ib
$(^{13}CONHCH_2)_2$		
3270	3274 w	
3155	3164 m	
3114 w	3126 sh	
3074 w		
3035 w	3044 sh	Mainly NH str
2999	3010 m	
2973	2960 w	
2955 w		
2909	2906 w	
2870	2862 w	
1700 sh		
1680	1678 sh	Impurity
1660	1657 vs	
1640	1638 sh	CO str
1528 vw	1524 vvw	
1485 sh		
1481 m	1474 m	NH ib
1463 w	1460 sh	
1455	1456 sh	
1447	1443 s	Ring str/CH_2 b
1438	1437 sh	
1410 vw	1407 vvw	
1348 sh		
1344	1341 s	CH_2 wag
1253	1250 w	CH_2 t
1072	1068 m	NC^{α} str
992	992 sh	
987	985 w	CH_2 r
913	912 m	Ring ib, ring str
851	836 s	NH ob
804	802 m	Ring ib, ring str
557	555 vvw	
545 vw	547 vvw	CO ob
449	446 s	CO ib
$(^{13}CONDCH_2)_2$		
2952 w	2952 vw	CH_2 as
2923 vw	2924 vvw	CH_2 ss
2464	2456 vw	
2385 vw	2380 sh	
2306 m	2317 s	ND str
2289 s	2292 m	
2236	2226 m	
2196	2190 sh	
1649	1648 vs	CO str
1625	1625 vs	
1504	1504 vvw	
1486 vw	1482 vvw	
1470	1470 sh	
1461	1460 sh	
1456	1456 sh	
1449	1447 s	Ring str/CH_2 b
1438	1437 sh	
1352	1347 s	CH_2 wag
1290 w	1290 vw	Impurity
1280 w	1280 vw	Impurity
1253	1251 w	CH_2 t
1228	1224 m	NC^{α} str, ND ib
1122	1117 vw	Impurity
1072	1067 vw	Impurity

Table 2. (continued)

LT	RT	Assign.
988	983 vw	CH_2 r
969	967 w	NC^{α} str, ND ib
915 w	911 vw	Impurity
900 w		Impurity
886	888 m	Ring ib
	866 vw	Impurity
	839 w	Impurity
780	774 w	Ring str
665	655 s	ND ob
511	503 w	CO ob
495 vvw		
447	443 s	CO ib

*Abbreviations: LT = low temperature; RT = room temperature: s = strong; m = medium; w = weak; v = very; sh = shoulder; str = stretch; as = antisym. str; ss = sym. str; b = bend; r = rock; t = twist; ib = in-plane bend; ob = out-of-plane bend; tor = torsion; / = overlap.

additional 35 cm^{-1} decrease. C-deuteration has little effect. Both NdDKP and NCdDKP show the factor group doublet expected, with splittings of 15 and 11 cm^{-1}; the higher frequency B_g component is much weaker than the A_g peak, and at LT the complex shifts downward by 2–3 cm^{-1}.

These changes reflect the effects of intramolecular and intermolecular interactions. The sizeable shift on *N*-deuteration in solution indicates a stronger coupling of CO str with NH ib than is present in *trans* peptides [22]. The factor group splitting arises from interactions between the two nonequivalent molecules in the unit cell; the magnitude of 15 cm^{-1} is unusually large for non-bonded forces. At first sight the drop of 50 cm^{-1} on crystallizing from solution might be attributed to the formation of the hydrogen bonds between translationally equivalent molecules along a chain. It is well known [23] that the formation of an X–H . . . Y–Z hydrogen bond results in a large (hundreds of cm^{-1}) decrease in the X–H stretch frequency and a considerably smaller drop for the Z–Y stretch. However, this cannot be the full explanation because the i.r. active CO str mode moves up from 1653 cm^{-1} in D_2O to 1668 cm^{-1} (average of the factor group pair) in solid NdDKP.

The Raman and i.r. active modes involve, respectively, in-phase and out-of-phase stretchings of the CO groups related by the inversion operation. (We note that in solution there is no overall coincidence of the Raman and i.r. spectra, so that the inversion symmetry persists.) The opposite directions of the shifts on

Table 4. Infrared frequencies (in cm^{-1}) of diketopiperazine in H_2O and D_2O at 48° C*

DKP/H_2O	NdDKP/D_2O	Assign.
	1653 s	CO str
1475 m	1475 w	Ring str
1456	1444 sh	CH_2 b
1331	1341 m	CH_2 wag
	995 vw	CH_2 r
1071 w		NC^{α} str
	964 w	NC^{α} str, ND ib
	879 w	Ring ib
	765 vw	Ring str

*Abbreviations: s = strong; m = medium; w = weak; v = very; sh = shoulder; str = stretch; b = bend; r = rock; ib = in-plane bend.

Table 3. Raman frequencies (in cm^{-1}) of diketopiperazine in H_2O and D_2O at 70°C*

$(CONHCH_2)_2/H_2O$	$(CONDCH_2)_2/D_2O$	Assign.
2993	3006 sh	
2930	2930 m	
2864 vw	2853 vvw	
2829	2820 vvw	
1675	1656 m	CO str
1640 sh		H_2O
1523	1510 m	Ring str
1443	1432 m	CH_2 b
1385 w		NH ib
1313	1324 m	CH_2 wag
1249	1249 w	CH_2 t
	1200 w	D_2O
1145 w		NC^{α} str
	969 w	NC^{α} str, ND ib
797	790 vs	Ring str
605 w	589 m	CO ib
546 vw	508 sh	CO ob
460	460 m	Ring ib
214	207 sh	Ring tor

*Abbreviations: s = strong; m = medium; w = weak; v = very; sh = shoulder; str = stretch; b = bend; t = twist; ib = in-plane bend; ob = out-of-plane bend; tor = torsion.

crystallizing indicate that there is a coupling between these CO groups. Since the *g-u* splitting is nearly zero in solution, the intramolecular coupling is correspondingly small. A possible intermolecular interaction may be mediated by the cyclic hydrogen bonding structure.

Large splittings of CO str modes have also been observed in dimers of carboxylic acids where there is a similar arrangement of an eight-membered centrosym-

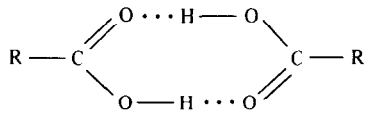

metric ring formed by hydrogen bonds. A normal coordinate calculation managed to reproduce this splitting in formic and acetic acids by introducing interaction force constants between coordinates [Δr(C=O), Δr(C–O), $\Delta\theta$(OCR), etc.] on the two monomers [24]. Tautomerism, in which the H atoms are transferred between the O atoms via a tunnelling process, resulting in chemically equivalent structures, was suggested as a possible cause of such interactions. Later, transition dipole coupling between C=O groups was proposed as an explanation [25]. In an *ab initio* calculation charge redistribution was shown to take place throughout the ring during the vibration of a C=O group, and this was offered as a mechanism for the interaction [26]. In DKP tautomerism is almost certainly ruled out because the X and Y atoms are different. In paper 2 [13] we will discuss the other two explanations in the light of our calculations.

While the CO str band in the *N*-deuterated compounds is sharp and of medium intensity, that in the NH molecules is weak and broad, and shows peculiar behavior. In the powder spectra the band consists of at least a doublet whose relative intensities change drastically at low temperature and on isotopic substitution. The single crystal spectra of DKP and CdDKP show an additional weaker band of B_g symmetry while the two more intense ones are both A_g and are strong in the same polarizations. We were unable to measure the B_g component in C13DKP because of poorer polarization.

These observations are most satisfactorily explained by the presence of a Fermi resonance interaction involving the A_g CO str component. For instance, the three peaks observed in the CO str region for DKP instead of the two expected indicate that one is a combination or overtone. The B_g component occurs by itself in the XY spectrum. The other two are both A_g and therefore satisfy the basic condition for Fermi resonance. Furthermore, they have the same polarization, XX (and YY as well), which would be the case if their intensity derived from one fundamental. The temperature behavior is exactly what is expected when one component of a Fermi resonance pair has a different rate or direction of change with temperature than the other, resulting in one component moving past the other [27]. Thus, at RT the unperturbed fundamental is at a higher frequency whereas at LT it is lower in frequency.

Similarly, the CdDKP and C13DKP spectra may be analysed by invoking Fermi resonance involving the A_g CO str. In CdDKP the interaction is weak at RT, but increases to virtually exact resonance at LT. In C13DKP the stronger peak remains on the low frequency side at both temperatures; the resonance at LT is extremely weak. Because of the basic similarity of the spectral features and the behavior of the resonance, it is reasonable to suppose that the A_g CO str is interacting with the same state in all three isotopic species.

We now proceed to a quantitative analysis of the Fermi resonance in order to obtain the unperturbed frequencies. Calling these ν_a and ν_b, and the perturbed (observed) values ν_+ and ν_-, the following relations can be derived [28]:

$$\nu_a = \tfrac{1}{2}\left[\nu_+ + \nu_- + \frac{(R-1)}{(R+1)}(\nu_+ - \nu_-)\right]$$

$$\nu_b = \tfrac{1}{2}\left[\nu_+ + \nu_- - \frac{(R-1)}{(R+1)}(\nu_+ - \nu_-)\right]$$

where R is the observed relative intensity, I_+/I_-. If we assume that ν_b is an overtone, the cubic coupling constant is [28] $K_{abb} = \pm[(\nu_+ - \nu_-)^2 - (\nu_a - \nu_b)^2]^{1/2}$. The integrated intensities in our spectra were obtained by resolving the overlapped bands. We assumed that the B_g band is of negligible intensity. This is shown by the single crystal spectra of the NH as well as ND molecules: much of the A_g intensity resides in the YY polarization whereas nearly all the B_g intensity is in the XY spectrum. This neglect of the B_g intensity is a poor approximation in the C13DKP LT spectrum where one of the A_g bands is very weak. We therefore did not analyse this spectrum; however, because of the weakness of the interaction the fundamental is probably shifted little from the observed peak at 1614 cm^{-1}.

The results of our analysis are presented in Table 5. To help in interpretation, we have listed the calculated unperturbed frequencies as ν_1 and ν_2 such that ν_1 is the frequency (either ν_a or ν_b) that is closer to the band of higher observed intensity in each case. Thus ν_1 is to be identified as the unperturbed A_g CO str. We also list $\nu_2/2$ and K_{122} in the expectation that ν_2 is an overtone. We checked that changes in R as large as $\pm 20\%$ caused changes of no more than ± 2 cm^{-1} in ν_1, ν_2 and K_{122}. On the other hand, changes in ν_+ and ν_- are more important, but these frequencies are much better determined.

We see that the Fermi resonance takes place between a ν_1 that shifts little on cooling (the slight decrease, if accurate, would be in line with the data on the N-deuterated compounds and consistent with an increase in the hydrogen bond strength) and a ν_2 that shows a significant increase at LT. The A_g–B_g splittings represented by the ν_1 values for DKP and CdDKP are 19 and 13 cm^{-1}, respectively, and are similar to the

Table 5. Fermi resonance analysis of CO stretch region in Raman spectra *

		ν_+	ν_-	I_+/I_-	ν_1	ν_2	$\nu_2/2$	$\lvert K_{122}\rvert$
$(CONHCH_2)_2$	RT	1652	1623	3.176	1645	1630	815	24.8
	LT	1666	1626	0.696	1642	1650	825	39.4
$(CONHCD_2)_2$	RT	1645	1613	4.474	1639	1619	810	24.7
	LT	1651	1620	1.0	1636	1636	818	31.0
$(^{13}CONHCH_2)_2$	RT	1632	1615	0.192	1618	1629	815	12.5
	LT	1651	1614	—	(1614)	—	—	—

*All units are cm^{-1} except for I_+/I_-.

splittings measured for NdDKP ($15\,cm^{-1}$) and NCdDKP ($11\,cm^{-1}$).

Turning to the origin of the ν_2 band, since it is of A_g symmetry it can only be an overtone or a combination of two fundamentals of the same species. (We assume only binary combinations and also do not consider $k \neq 0$ modes.) The large LT shift makes the overtone of NH ob the most likely candidate. The NH ob mode has the largest LT shift in the mid-frequency region, indicating high anharmonicity of the mode. It also decreases by about $10\,cm^{-1}$ from DKP to CdDKP and by only $1\,cm^{-1}$ from DKP to C13DKP; both these shifts are consistent with the changes in ν_2. We cannot be sure whether ν_2 is the overtone of the Raman active or the i.r. active NH ob mode, but at least in DKP the LT shift of $19\,cm^{-1}$ of the i.r. band seems to be too large.

Having the unperturbed A_g CO str frequencies in hand, we obtain the shifts of this band on N-deuteration at RT: DKP ($43\,cm^{-1}$), CdDKP ($37\,cm^{-1}$), and C13DKP ($52\,cm^{-1}$). The large contribution of NH ib that these shifts imply explains the low intensity of the CO str complex in the crystalline NH molecules.

The three other modes in the mid-frequency region involving in-plane vibrations of the peptide group, CN str, NH ib and CO ib, are placed at 1519, 1457 and $612\,cm^{-1}$, respectively, in DKP, all of which are a_g bands.

The $1519\,cm^{-1}$ band shifts to $1472\,cm^{-1}$ in NCdDKP, where it is the only one left in the $1400\,cm^{-1}$ region. As we will see later, it is more appropriately characterized as an out-of-phase stretching of the C^α–C–N group. This mixing with $C^\alpha C$ str is reflected in the sizeable shifts on *C*-deuteration. The smaller shifts on *N*-deuteration and the higher Raman intensity as compared to the *trans* amide II mode, indicate less coupling with NH ib. Finally, the observation of a CN str mode at $1519\,cm^{-1}$ means that one of the commonly invoked criteria for identification of a *cis* peptide, viz. the absence of a band corresponding to amide II in the $1500\,cm^{-1}$ region [29, 30], is not always valid. It remains to be seen whether this feature is peculiar to DKP or is a characteristic of *cis* peptides, or at least of a certain class of *cis* peptides.

The $1457\,cm^{-1}$ band in DKP disappears on N-deuteration. Its large intensity probably results from coupling of NH ib with CH_2 bend: it is weaker and broader in CdDKP where it drops to $1437\,cm^{-1}$. (The $200\,cm^{-1}$ band may be used as an internal intensity standard in the solid state spectra.) In Cl3DKP the 1451 and $1412\,cm^{-1}$ bands are nearly equal in intensity, suggesting stronger mixing of NH ib and CH_2 bend. In NdDKP the pure ND ib mode would be expected to be near $1100\,cm^{-1}$. Interaction with NC^α str gives rise to the two bands at 1241 and $1008\,cm^{-1}$. In NCdDKP these two bands shift up to 1284 and $1110\,cm^{-1}$, probably as a result of mixing with CD_2 wag (which shifts by $50\,cm^{-1}$ from CdDKP to NCdDKP). In H_2O solution NH ib is weaker and is at a much lower frequency than in the crystal. This mode is therefore highly sensitive to the hydrogen bond. The $969\,cm^{-1}$ band in D_2O is probably one member of the NC^α str–ND ib pair; its partner is too weak to be seen or is overlapped with D_2O bend near $1200\,cm^{-1}$.

The CO ib mode, at $612\,cm^{-1}$, is one of the strongest peaks, unlike the amide IV mode in poly(glycine I) [31, 32]. Its shift on *C*-deuteration is much less than that of the other a_g band at $795\,cm^{-1}$, allowing the assignment of the latter to $C^\alpha C$ str. ^{13}C-substitution has little effect on its position and, unlike NH ib, it shifts only slightly in solution.

The out-of-plane vibrations of the peptide group, NH ob, CO ob and CN torsion, give rise to the bands at 832, 561 and $236\,cm^{-1}$, respectively, in DKP. These bands are all stronger in the b_g than in the a_g spectra.

The $832\,cm^{-1}$ peak is attributed to NH ob because of its shift to $626\,cm^{-1}$ in NdDKP. It sharpens dramatically and moves up by $12\,cm^{-1}$ at LT. It is not observed in solution.

In contrast to CO ib, the CO ob mode shows a significant ^{13}C shift. It drops to $537\,cm^{-1}$ in NdDKP, probably as a result of coupling with ND ob, this being evidenced by the reduced intensity at $537\,cm^{-1}$ and the enhanced intensity at $626\,cm^{-1}$. The large decrease ($57\,cm^{-1}$) on *C*-deuteration suggests interaction with CD_2 rock.

As we will see in paper 2 [13], the mode in the $200\,cm^{-1}$ region is more properly described as a ring torsion rather than CN torsion alone. This band is

broad and shifts little on *N*-deuteration or ^{13}C-substitution, but drops by 28 cm^{-1} on *C*-deuteration. It is seen near 214 cm^{-1} in H_2O solution.

Vibrations of methylene group. The methylene bend, wag, twist and rock modes are assigned on the basis of their deuteration shifts and polarization. The CH_2 bend mode shows a 7 cm^{-1} factor group splitting in NdDKP. Its A_g component has nearly all its intensity in the *YY* polarization. As noted earlier, CH_2 bend in C13DKP appears to be strongly mixed with NH ib, resulting in a much reduced intensity. Also, in DKP the 1457 cm^{-1} band shifts more at LT than that at 1422 cm^{-1}, but in C13DKP the 1412 cm^{-1} band is more sensitive to temperature than that at 1451 cm^{-1}. The CD_2 bend mode is insensitive to *N*-deuteration.

Like CH_2 bend, CH_2 wag shows a_g polarization. It also shows significant splitting; the B_g component is intense enough for the doublet nature to be obvious even in the powder spectra. In CdDKP CD_2 wag is very weak and is situated close to CD_2 twist, forming a triplet near 950 cm^{-1}. Nevertheless, all three bands are unambiguously identified by their polarization, the CD_2 wag doublet showing in-plane and A_g or B_g polarization whereas CD_2 twist is out-of-plane. In NCdDKP the CD_2 wag pair are again located by means of the single crystal spectra. Their large shift (50 cm^{-1}) from CdDKP may result from coupling with NC^{α} str and ND ib, as mentioned earlier.

The CH_2 twist mode is of b_g symmetry. It appears to be rather pure, showing little change on *N*-deuteration or ^{13}C-substitution and a CH_2 to CD_2 frequency ratio of 1.34.

The weak band near 980 cm^{-1} in DKP and NdDKP does not show distinct a_g or b_g character. It is therefore assigned to CH_2 rock on the basis of elimination, deuteration shift and proximity to the i.r. active CH_2 rock. Its shift of 8 cm^{-1} on ^{13}C-substitution indicates interaction with CO ob. The polarization of the 870 cm^{-1} band in the *C*-deuterated materials is more clearly b_g.

Skeletal vibrations. Besides the peptide CN str and the ring torsion, there are four other Raman active vibrations of the ring skeleton: NC^{α} str, $C^{\alpha}C$ str and two ring angle deformations. All four modes are in-plane. The NC^{α} str mode near 1150 cm^{-1} in DKP shows a 6 cm^{-1} splitting. Its position in the deuterated materials is very different in all cases. In NdDKP it interacts with ND ib and in CdDKP it seems to be mixed with CD_2 wag. In NCdDKP it may be interacting with both ND ib and CD_2 wag.

The very strong band at about 790 cm^{-1} in DKP and NdDKP shifts appreciably on *C*-deuteration and is assignable to $C^{\alpha}C$ str. However, its negligible shift on ^{13}C-substitution suggests that it arises from the in-phase stretching of the C^{α}–C–N group, in which the motion of the carbonyl carbon is very small. The implication then is that the band in the 1500 cm^{-1} region, which does shift by 18 cm^{-1} from DKP to C13DKP, is the out-of-phase stretching of $C^{\alpha}CN$. Thus there seems to be a strong coupling between the CN and $C^{\alpha}C$ stretches.

Finally, the ring angle bends are assigned to the two a_g bands whose positions in the 400 cm^{-1} region are quite constant in the isotopic series. However, we cannot be more specific about the nature of either one at this point. They do show some differences in polarization: one is strongest in *XX* and the other apparently in *YY*. There are subtle differences in their intensity changes on isotopic substitution. Only one of them is observed in solution (we are not sure which one), and the higher frequency band is noticeably split in the solid state spectra.

Infrared in mid-frequency region

Vibrations of CONH group. The CO str mode is clearly the very intense band in the 1600 cm^{-1} region. It shows the expected factor group doublet in all spectra and especially in those of the deuterated samples. In the LT spectrum of DKP and in the spectra of the *C*-deuterated compounds an additional component is observed. The shoulders on the high frequency side of the C13DKP band are probably due to ^{12}C impurities.

In those cases where only a doublet appears, the higher frequency component is more intense, except in NdC13DKP where the pair are almost equally strong and show the most distinct splitting. In NdDKP and the ^{13}C samples the positions of the doublet change very little at LT, and there is some sharpening of the bands. In DKP the doublet at RT gives way at LT to two relatively sharp bands of nearly equal intensity and a shoulder on the lower frequency component. The 1712 cm^{-1} band seems to have shifted from 1697 cm^{-1}. Such large changes in appearance and position on cooling are in direct contrast to the NdDKP and ^{13}C spectra.

A possible explanation is that a Fermi resonance interaction occurs in DKP at LT. This seems to involve the 1697 cm^{-1} band, resulting in the strong 1712 cm^{-1} peak and the 1692 cm^{-1} shoulder. The redistribution of intensity causes the 1712 cm^{-1} peak to be weaker than that at 1697 cm^{-1}. The 1678 cm^{-1} band moves only slightly, to 1682 cm^{-1}, consistent with the small changes seen in the other spectra.

To analyse this resonance in detail would require resolution of the band contour. We will not pursue this here since we do not need the LT frequencies for our force field calculations. However, it is most likely that a combination of the Raman active NH ob with its i.r. active counterpart is responsible. At RT the position of this combination (which may be either A_u or B_u) is $832 + 837 = 1669\ cm^{-1}$, but at LT the value is $844 + 856 = 1700\ cm^{-1}$, thus accounting for the presence of the interaction only at LT. In the *C*-deuterated materials Fermi resonance appears to be at work also, though the changes at LT are not as drastic as in DKP. We will not analyse the resonance in these spectra.

Thus, at RT we may use the band positions of CO str

from DKP, NdDKP and the ^{13}C molecules. The factor group splittings are about 20–25 cm^{-1}, slightly more than in the Raman spectra. The best-defined splitting, that of NdC13DKP, hardly changes at LT. On *N*-deuteration the mean position of the doublet shifts by 20 cm^{-1} for DKP and 10 cm^{-1} for C13DKP, considerably less than the Raman bands. Also, unlike the Raman, the i.r. bands tend to move upward on cooling. This suggests that the LT downward shifts in the Raman spectra may not be due directly to an increase in hydrogen bond strength, but are caused by a change in the same mechanism that is responsible for the *g-u* splitting.

It is not possible to tell which component of the doublet belongs to which species (A_u or B_u). Such a determination requires observation of a $(10\bar{1})$ section; the A_u component will have polarization along *b* and the B_u along [101]. The spectra of NEWMAN and BADGER [1] indicate that the B_u band is more intense than the A_u (even though the absorption is saturated in both polarizations). This would imply that the higher frequency component seen in our spectra is B_u. It is noteworthy that the components of the A_u–B_u pair in NdC13DKP are of almost equal intensity, indicating a significant difference in the transition moments, and therefore in the nature of the normal mode, as compared to DKP, NdDKP and C13DKP.

Finally, we may note that in D_2O solution the CO str band is a sharp singlet. Interestingly, the position of this mode in a non-hydrogen bonding solvent, DMSO, is almost the same for DKP and NdDKP (1684 and 1682 cm^{-1}). Similar observations on the *trans* amide I mode were made by BEER *et al.* [33] in their studies of small amides.

The 1400 cm^{-1} region has been the subject of controversy. Two peptide group vibrations, CN str and NH ib, are expected in this region, as is CH_2 bend. The problem has been that only two bands have been observed, so that various schemes of overlap had to be assumed. Our data conclusively establish the positions of all three modes.

The third band is most clearly revealed in the C13DKP spectra, where the strong 1470 cm^{-1} band of DKP is shifted down to 1443 cm^{-1}. This band, at 1474 cm^{-1}, which shows an upward shift of 7 cm^{-1} at LT, disappears in NdC13DKP; it is therefore NH ib. It is also seen in DKP as a shoulder at 1482 cm^{-1} at RT, and it sharpens and shifts to 1493 cm^{-1} on cooling, allowing it to be resolved from its stronger neighbor. The 1470 cm^{-1} band in DKP, which remains at 1462 cm^{-1} in NCdDKP, is evidently CN str. The 1445 cm^{-1} band disappears in CdDKP and is easily assigned to CH_2 bend.

In addition to the three major peaks, we also observe several much weaker features in this region whose origins are not completely clear. Probably most or all of them may be combinations or overtones. If the shoulders on each main band are in Fermi resonance with the latter, the resonance is weak and the positions of the fundamentals are not likely to be shifted by more than a few cm^{-1}. If a shoulder is a factor group component, the splitting is small and we will not be greatly in error in using the position of the stronger partner in our refinement of an intramolecular force field. We therefore do not attempt a detailed assignment of these features in this work.

The CN str mode drops by less than 10 cm^{-1} on deuteration from DKP to NCdDKP, compared to the 47 cm^{-1} decrease in the Raman. On the other hand, the ^{13}C shift is much larger for the i.r. mode (37 vs 18 cm^{-1}). From our discussion of the Raman CN str and $C^{\alpha}C$ str modes we may expect a similar mixing in the i.r., so that the 1470 cm^{-1} band is probably due to an out-of-phase stretch of $C^{\alpha}CN$.

The 49 cm^{-1} difference between the i.r. and Raman CN (or out-of-phase $C^{\alpha}CN$) str in DKP is quite large. Unlike the CO stretches, however, this splitting already exists in solution (H_2O and D_2O), and is therefore largely of intramolecular origin. It is interesting that in NCdDKP the separation of these bands is only 10 cm^{-1}, with values close to that of the amide II mode in perdeutero-polyglycine ($\sim$ 1460 cm^{-1}) [22]. The removal of couplings with NH ib and CH_2 bend may account for this observation.

The NH ib mode shows a significant LT shift. It is hardly affected by *C*-deuteration, in contrast to the 20 cm^{-1} decrease in its Raman counterpart, indicating less mixing with CH_2 bend. In NdDKP the ND ib interacts with NC^{α} str, resulting in the 1235 and 969 cm^{-1} bands. This is similar to what happens in the Raman.

Thus, the observation of CN str and NH ib in the 1400 cm^{-1} region in DKP is consistent with the usual expectation that a *cis* peptide group has no band in the 1500 cm^{-1} region, though this is not true of the Raman spectrum of DKP. The fact that the bands due to CN str and NH ib are so close together in DKP is, of course, a result of their negligible interaction; in *trans* peptides their coupling gives rise to the amide II and III modes with a 200 cm^{-1} separation.

The remaining in-plane CONH vibration, the CO ib, is assigned to the strong band at 447 cm^{-1}. The early single crystal studies [1, 2] did not measure the region below 700 cm^{-1}. However, our observations using an (010) section clearly show this band to be in-plane. The high intensity of CO ib in DKP, in i.r. absorption as well as in Raman scattering, contrasts with its weakness in poly(glycine I) [31].

Turning to the out-of-plane vibrations of the peptide unit in this region, the NH ob mode is easily assigned to the broad, strong band at 837 cm^{-1}, which is known to have out-of-plane dichroism and which disappears on N-deuteration. It shows a large increase in frequency and sharpness at LT, like the Raman active NH ob mode. Also similar to the Raman mode, it shifts by about 10 cm^{-1} on *C*-deuteration, possibly because of coupling with CD_2 rock.

The CO ob mode has not been assigned reliably

before. The weak but distinct band at 510 cm^{-1} in NdDKP was left unassigned by ASAI *et al.* [6]. It shows a ^{13}C shift of 7 cm^{-1}. In NCdDKP it drops to 460 cm^{-1}, a band which shows out-of-plane dichroism in our single crystal measurements. We therefore assign this band to CO ob. The corresponding CO ob absorption in DKP appears to be at 553 cm^{-1}, moving to 547 cm^{-1} in C13DKP and to 485 cm^{-1} in CdDKP. The marked differences in intensity between the CO ob mode in DKP and C13DKP on the one hand and in the deuterated molecules on the other can be explained by interaction of CO ob with ND ob. For instance, on N-deuteration the 837 cm^{-1} band in DKP drops to 661 cm^{-1}. This represents an NH : ND frequency ratio of only 1.266. A mixing with CO ob, resulting in the 661 and 510 cm^{-1} bands, is therefore indicated. The ^{13}C shift of the 510 cm^{-1} band is similar to that for the well-assigned Raman CO ob. Furthermore, whereas the NH ob in DKP is insensitive to ^{13}C-substitution, the 661 cm^{-1} band in NdDKP decreases by 6 cm^{-1} in NdC13DKP. A further 50 cm^{-1} shift of the 510 cm^{-1} band on C-deuteration is probably caused by coupling with CD_2 rock as well. Thus CO ob is satisfactorily assigned in the deuterated materials, where its intensity is enhanced. Since the 510 cm^{-1} band in NdDKP appears to have resulted from the 553 cm^{-1} band in DKP, this latter peak may be attributed to CO ob.

Vibrations of methylene group. As we have already noted, CH_2 bend appears at 1445 cm^{-1} in DKP. It is insensitive to temperature or *N*-deuteration and becomes overlapped with CN str in the ^{13}C molecules. The CD_2 bend mode is near 1070 cm^{-1}; in NCdDKP at LT it is a doublet with a spacing of 4 cm^{-1}.

The CH_2 wag mode at 1343 cm^{-1} in DKP disappears on C-deuteration. In CdDKP it is mixed with NC^{α} str in the bands at 1189 and 1005 cm^{-1}, in view of the large change in the 1075 cm^{-1} band in DKP.

The CH_2 twist mode is easily assigned to the 1252 cm^{-1} band, as other workers have done. The CD_2 twist mode is placed at 930 cm^{-1}; this band shows out-of-plane dichroism in our single crystal spectra of NCdDKP. Like its Raman counterpart, the i.r. methylene twist is highly insensitive to *N*-deuteration or ^{13}C-substitution.

The weak CH_2 rock absorption at 993 cm^{-1} in DKP is also not shifted significantly on *N*-deuteration, but in the ^{13}C molecules it drops by about 10 cm^{-1}, possibly because of coupling with CO ob. The CD_2 rock assignment is not clear cut. As in the Raman spectrum, it is expected to be in the 800 cm^{-1} region. In CdDKP the bands at 885 and 843 cm^{-1} seem to be the only possibilities, but the high i.r. intensity of both presents a puzzle. One of them is expected to be the ring ib, but unfortunately our single crystal spectra are not conclusive: it is not clear which band is out-of-plane. At LT while the NH ob mode moves 10 cm^{-1} to 837 cm^{-1}, the 843 cm^{-1} band hardly shifts. At the same time, the 885 cm^{-1} band shows an increase in intensity and in frequency. These observations point to an interaction of NH ob with the 885 cm^{-1} band and not with that at 843 cm^{-1}. Since it is more likely for two out-of-plane vibrations to be coupled, we tentatively assign CD_2 rock at 885 cm^{-1} in CdDKP.

In NCdDKP the 800 cm^{-1} region becomes even more complicated with the presence of NC^{α} str. There are two main bands, at 838 and 890 cm^{-1}. Of the several weak features in the 800–1000 cm^{-1} region, an 872 cm^{-1} band is the only one that cannot be definitively assigned to impurities; it is stronger than in the refluxed material. Our tentative conclusion then is as follows. The CD_2 rock mode is at 872 cm^{-1}, its much reduced intensity being a consequence of the absence of NH ob mixing; this places it close to the Raman CD_2 rock mode, a similar situation to that seen with the CH_2 rocks. The ring ib mode is at 838 cm^{-1} while the NC^{α} str mode (coupled with ND ib and possibly CD_2 wag) appears at 890 cm^{-1}.

Skeletal vibrations. Besides the CN str, there are three vibrations of the ring skeleton above 400 cm^{-1} in the i.r. The NC^{α} str mode is located at 1075 cm^{-1} in DKP. In NdDKP, as we noted earlier, it is coupled with ND ib, and in CdDKP it mixes with CD_2 wag to give the 1189 and 1005 cm^{-1} bands. In NCdDKP an additional coupling with ND ib causes the 1005 cm^{-1} band to move (probably) to 890 cm^{-1}.

The 913 cm^{-1} band in DKP has been assigned by others to $C^{\alpha}C$ str while the 805 cm^{-1} band was considered to be the ring ib mode. Our calculations indicate that these two bands are mixtures of ring ib and the in-phase $C^{\alpha}CN$ str. The small ^{13}C shifts are consistent with this description, and in particular with the notion that $C^{\alpha}C$ str cannot be involved by itself without an accompanying in-phase stretching of the adjacent CN bond. In the deuterated materials our calculations show that the coupling of ring ib and $C^{\alpha}CN$ str is reduced, with the $C^{\alpha}CN$ str mode dropping to the 700 cm^{-1} region while the ring ib mode remains in the 800 cm^{-1} region.

High frequency region

Although only one NH and two CH str modes are expected in the Raman or i.r. spectra in this region, the spectra show remarkable complexity. Since effects such as Fermi resonance are undoubtedly at work, we will not analyse this region fully but will merely try to extract reasonable values for the CH and NH str frequencies.

The Raman active CH str and CD str modes are amenable to more complete analysis than the other modes; we therefore consider these modes first. In NdDKP, where the NH str bands are absent, the 2800–3000 cm^{-1} region shows two main bands with a smaller one at 2826 cm^{-1}. The 2954 cm^{-1} band is clearly the CH_2 antisymmetric stretch (CH_2 as) since it is predominantly b_g. The other two bands are both strong in the *ZZ* spectrum, which suggests that they are due to a Fermi resonance of the CH_2 symmetric stretch (CH_2 ss) with an overtone or combination of A_g symmetry. The interaction is small in view of the large

intensity difference. In DKP the resonance is even weaker, with the less intense band shifting to 2835 cm^{-1} and the stronger one moving to 2929 cm^{-1}. We can therefore take CH_2 ss to be at 2929 and CH_2 as to be at 2954 cm^{-1}.

In CdDKP the 2100–2300 cm^{-1} region has at least five bands. Four of these are associated with each other and probably derive their intensity from CD_2 ss, while the fifth, at 2222 cm^{-1}, is quite clearly the unperturbed CD_2 as mode since it alone is strong in the ZY spectrum. In the CD_2 ss complex, which is mainly A_g, the bands at 2114 and 2163 cm^{-1} dominate. As a first approximation, we can assume a two-level resonance involving just these two peaks. Taking the relative intensity $I(2163)/I(2114) \approx 0.5$, we derive the unperturbed frequencies as 2130 and 2147 cm^{-1}. The CD_2 ss mode is therefore at about 2130 cm^{-1} in CdDKP.

Though we expect the CD str modes to be unchanged in frequency in NCdDKP, it is instructive to analyse the NCdDKP spectra to check for consistency. Here we find four major bands besides the ND str at 2290 cm^{-1}. The two at 2112 and 2157 cm^{-1} are both strong in the XX and ZZ spectra while the other two both show ZY polarization. The first pair is easily assigned to CD_2 ss and the second pair to CD_2 as. Since the intensities of the 2112 and 2157 cm^{-1} bands are nearly equal (at RT), we obtain immediately the common unperturbed frequency: 2135 cm^{-1}. If we take the relative intensity of the other pair as $I(2230)/I(2201) \approx 2$, the resulting unperturbed frequencies are 2220 and 2211 cm^{-1}. The CD stretches in NCdDKP are therefore at about 2135 and 2220 cm^{-1}, in good agreement with the values derived independently for CdDKP.

The two i.r. active CH modes are extremely weak. They are best seen in NdDKP and NdC13DKP, where they appear at 2922 and 2952 cm^{-1}. These peaks do not seem to be perturbed by Fermi resonance. The CH_2 as band at 2952 cm^{-1} shows out-of-plane dichroism in our single crystal spectra of NdDKP. It is also seen in the single crystal spectra of DKP, confirming the findings of AMBROSE *et al.* [3] and disagreeing with ASAI *et al.* [6] who placed CH_2 as at 2986 cm^{-1} in DKP; we do not think the CH stretches are resolvable from the NH complex in the powder spectra.

The CD str modes are stronger, but are also more complicated. A band at 2220 cm^{-1} in CdDKP is close to the 2222 cm^{-1} Raman band assigned as unperturbed CD_2 as. Of the other three prominent bands in this region, 2078, 2110 and 2176 cm^{-1}, none corresponds to the Raman active CD_2 ss calculated at 2130 cm^{-1}. In NCdDKP a band at 2228 cm^{-1} may be attributed to CD_2 as in view of its agreement with the position of the Raman mode; whether it is perturbed or not is unclear. The three bands at 2080, 2110 and 2154 cm^{-1} match closely the components of the CD_2 ss complex in the Raman.

The NH and ND str bands in the 3000 and 2300 cm^{-1} regions are extremely complex. Looking at the i.r. NH str mode, one is struck by the large number of peaks extending over a range of 400 cm^{-1}. The ND str mode is somewhat simpler, with fewer bands in a narrower (150–200 cm^{-1}) region, and is much reduced in overall intensity. There are subtle changes on ^{13}C-substitution and more obvious differences on *C*-deuteration.

At LT the bands forming each complex sharpen appreciably, revealing even more fine structure. In addition, some peculiar shifts occur. In the NH region the peaks above 3000 cm^{-1} shift downward while peaks below 3000 cm^{-1} shift upward. The most intense band in the ND complex has a shoulder. In NdDKP and NdC13DKP this shoulder is on the low frequency side at RT, but it appears on the high frequency slope at LT. In NCdDKP the shoulder is on the high frequency side at both temperatures. In all three cases the strong band shifts down by 20–30 cm^{-1} at LT.

The Raman active NH str mode is diffuse, extending from 3200 to nearly 2800 cm^{-1}. The ND str mode is dominated by a strong, broad band at about 2290 cm^{-1} which decreases by about 10 cm^{-1} on cooling. It is apparent that the ND str mode has the simplest structure. We may therefore take 2290 cm^{-1} as a reasonable value for the ND str fundamental.

As a final observational note, we may point out the weak i.r. bands in the NH str region in the *N*-deuterated materials. These are due to residual NH absorption; with increasing concentration of NH molecules the peaks become progressively similar to those of the pure NH samples. It is interesting that even at very low concentrations the NH complex already shows its principal features: the large number of individual peaks over a wide frequency range. However, the relative intensities of these peaks do change as the concentration increases (compare, for example, the LT spectra of CdDKP and NCdDKP).

We will not try to explain these spectra in detail. Spectra similar to ours are often observed in other hydrogen bonded systems and considerable effort has been made to understand them in the belief that such distinctive features reflect fundamental properties of the hydrogen bond [34, 35]. There are two explanations that appear applicable to our spectra. In one, the numerous sub-bands of the XH stretch complex are attributed to Fermi resonance. In the other, anharmonic coupling of the XH stretch with low frequency modes of the XH . . . YZ group, such as the H . . . Y stretch (of about 100–200 cm^{-1} in frequency), is considered to result in sum and difference frequencies of the form $\nu_{XH} \pm n\nu_l$. This second theory has been put in a quantitative form [36]. Spectra of systems such as carboxylic acid dimers and crystals, which are very similar to DKP in their hydrogen bond configuration, have been fitted remarkably well. The extensive fine structure, the relative intensities of individual peaks and the marked narrowing of the complex on deuteration were all satisfactorily reproduced [37].

By contrast, quantitative explanations based on

Fermi resonance are seldom attempted because of the difficulty of solving a many-level resonance scheme (see, however, [28]). Spectra are then considered to be "explained" if combinations or overtones can be found that are close to the sub-band maxima. One problem with this is that the interaction among several levels can cause unexpectedly large shifts. On the other hand, the changes in the XH stretch complex when neighboring atoms are substituted, such as in CD_3COOH and CdDKP, are difficult to account for if only coupling with the low frequency modes is considered since these modes would hardly be affected by the substitution.

It seems then that a more complete explanation would include both types of coupling [35, 36]. The ν_{XH}–ν_l coupling, which presumably is always present to a certain extent, spreads out the XH stretch band, making possible a larger number of Fermi resonance interactions with combinations and overtones. In addition, in crystals like DKP the resonant interaction between nearby hydrogen bonds can modify the complex even further [37].

Low frequency region

There are six Raman active rotatory lattice vibrations: three A_g and three B_g. The spectra apparently show only five peaks below $200\,cm^{-1}$. Since the single crystals allow us to scan down to less than $5\,cm^{-1}$ from the Rayleigh line, it is improbable that there are any other undetected bands. We believe the sixth band is overlapped at $126\,cm^{-1}$ (all values are for DKP). The peak at $126\,cm^{-1}$ shows appreciable intensity in both $A_g(XZ)$ and $B_g(ZY)$ polarization. We do not think this can be attributed to depolarization errors, which can be seen to be very small for the other four bands. Furthermore, the $126\,cm^{-1}$ band in the powder spectrum is noticeably broader than the others, but its width in the polarized spectra is in each case comparable to those of the others.

The assignment of the symmetry species of the other four bands is straightforward. The 51 and $142\,cm^{-1}$ bands clearly have most of their intensity in the *YY* polarization. We see no reason for assigning the 126 and $142\,cm^{-1}$ bands to overtone or combination transitions, as STEIN did [8].

In the i.r. region below $400\,cm^{-1}$ we expect two ring torsional vibrations and the three translatory lattice vibrations. The far i.r. spectra at RT show the two peaks at 177 and $148\,cm^{-1}$ noted by SHIMANOUCHI and HARADA [5], who assigned them both to the torsional modes. In addition, a weak band at $83\,cm^{-1}$ and an even weaker one at $47\,cm^{-1}$ are seen. We are not sure what the broad feature near $63\,cm^{-1}$ is. The $83\,cm^{-1}$ band sharpens slightly at LT and moves to $88\,cm^{-1}$. The LT effect on the 148 and $177\,cm^{-1}$ bands is dramatic. Both sharpen and move upward by about $10\,cm^{-1}$, and their relative intensity becomes more equal. The $148\,cm^{-1}$ band splits into at least three components; it is probable that this structure is present at RT also since a slight shoulder is discernible on the low frequency slope.

Our preliminary calculations indicate that the two A_u lattice modes are well below $100\,cm^{-1}$ and the B_u mode is above. We therefore tentatively assign the 47 and $83\,cm^{-1}$ peaks to the A_u modes, and the B_u mode is placed at $148\,cm^{-1}$. The $177\,cm^{-1}$ band is then one of the ring torsions while the other ring torsion is assigned to an unobserved band near $285\,cm^{-1}$, which is, however, clearly seen in the inelastic neutron scattering study of DKP [38].

Our argument for this last assignment is as follows. Looking at the results of the neutron scattering work, it is possible to correlate, to within $20\,cm^{-1}$, each neutron peak with an observed i.r. or Raman band, except for one of the pair at 215 and $285\,cm^{-1}$. The $570\,cm^{-1}$ peak, for instance, can be matched with either the i.r. or Raman CO ob mode. (We think that BOUTIN and YIP's value of $168\,cm^{-1}$ for one of their peaks is in error; their spectrum shows a shoulder near 190 which is, however, still in fair agreement with the $177\,cm^{-1}$ i.r. band.) Both the 215 and $285\,cm^{-1}$ neutron peaks are distinctly present. Our calculations show that both the Raman ring torsion and the i.r. higher frequency torsional mode involve large motions of the hydrogen atoms and are therefore consistent with the high neutron intensity. Because we observe the Raman ring torsion at $236\,cm^{-1}$, we correlate it with the $215\,cm^{-1}$ band. This leaves the $285\,cm^{-1}$ band to be assigned to the i.r. ring torsion, there being no other observed fundamental in the 200–400 cm^{-1} region.

Without more data (particularly on polarization), it is difficult to account for the multiplet structure of the $150\,cm^{-1}$ band. A Fermi resonance with the combination of the $67\,cm^{-1}$ Raman band and the $83\,cm^{-1}$ i.r. band is a possibility. A peculiar doubling of the H . . . O stretch mode near $180\,cm^{-1}$ has been observed in dimers of acetic acid [36]. This has been explained as being due to a ν_{XH}–ν_l coupling analogous to that affecting the XH stretch mode. It is clear that our assignments for the far i.r. region are the weakest aspect of our experimental results. More data would be helpful.

CONCLUSIONS

The availability of DKP and five of its isotopic derivatives, plus polarized Raman spectra on single crystals as well as Raman and i.r. spectra in the powder and solution states, has made possible an essentially complete assignment of the Raman and i.r. bands of this molecule in the crystalline state. This assignment provides necessary information for refining an intramolecular force field for DKP [13], which can serve as a model for vibrations of the *cis* peptide group.

Acknowledgements—This research was supported by National Science Foundation grants PCM-7921652 and DMR-7800753. We are indebted to Dr. JOHN F. RABOLT for obtaining the far i.r. spectra.

REFERENCES

[1] R. NEWMAN and R. M. BADGER, *J. chem. Phys.* **19**, 1147 (1951).
[2] T. SHIMANOUCHI, K. KURATANI and S. I. MIZUSHIMA, *J. chem. Phys.* **19**, 1479 (1951).
[3] E. J. AMBROSE, A. ELLIOTT and R. B. TEMPLE, *Proc. R. Soc.* **A206**, 192 (1951).
[4] T. MIYAZAWA, *J. Molec. Spectrosc.* **4**, 155 (1960).
[5] T. SHIMANOUCHI and I. HARADA, *J. chem. Phys.* **41**, 2651 (1964).
[6] M. ASAI, K. NODA and A. SADO, *Spectrochim. Acta* **30A**, 1147 (1974).
[7] H. S. RANDHAWA, S. HARTO and W. WALTER, *Appl. Spectrosc.* **31**, 468 (1977).
[8] P. B. STEIN, Ph.D. Thesis, University of Oregon (1973).
[9] K. FUKUSHIMA, Y. IDEGUCHI and T. MIYAZAWA, *Bull. chem. Soc. Japan* **37**, 349 (1964).
[10] S. KARPLUS and S. LIFSON, *Biopolymers* **10**, 1973 (1971).
[11] R. DEGEILH and R. E. MARSH, *Acta crystallogr.* **12**, 1007 (1959).
[12] P. SENGUPTA, S. KRIMM and S. L. HSU, *Biopolymers* **23**, in press (1984).
[13] T. C. CHEAM and S. KRIMM, *Spectrochim. Acta* **40A**, 503 (1984).
[14] J. P. GREENSTEIN and M. WINITZ, *Chemistry of the Amino Acids*, Vol. 2. John Wiley, New York (1961), illustrative procedures 10–3 and 10–51.
[15] R. B. COREY, *J. Am. chem. Soc.* **60**, 1598 (1938).
[16] J. C. WARD, *Proc. R. Soc.* **A228**, 205 (1955).
[17] S. L. HSU, Ph.D. Thesis, University of Michigan (1975).
[18] T. R. GILSON and P. J. HENDRA, *Laser Raman Spectroscopy*. John Wiley, London (1970).
[19] R. RAMANI, V. SASISEKHARAN and K. VENKATESAN, *Int. J. Peptide Protein Res.* **9**, 277 (1977).
[20] K. LONSDALE, *Acta crystallogr.* **14**, 37 (1961).
[21] M. SUZUKI, T. YOKOYAMA and M. ITO, *Spectrochim. Acta* **24A**, 1091 (1968).
[22] S. SUZUKI, Y. IWASHITA, T. SHIMANOUCHI and M. TSUBOI, *Biopolymers* **4**, 337 (1966).
[23] G. C. PIMENTEL and A. L. MCCLELLAN, *The Hydrogen Bond*. Freeman, San Francisco (1960).
[24] S. KISHIDA and K. NAKAMOTO, *J. chem. Phys.* **41**, 1558 (1964).
[25] S. KRIMM and Y. ABE, *Proc. natn. Acad. Sci. U.S.A.* **69**, 2788 (1972).
[26] P. BOSI, G. ZERBI and E. CLEMENTI, *J. chem. Phys.* **66**, 3376 (1977).
[27] S. LEWIS and W. F. SHERMAN, *Spectrochim. Acta* **35A**, 613 (1979).
[28] G. DELLAPIANE, S. ABBATE, P. BOSI and G. ZERBI, *J. chem. Phys.* **73**, 1040 (1980).
[29] L. J. BELLAMY, *Infrared Spectra of Complex Molecules*. John Wiley, New York (1975).
[30] H. E. HALLAM and C. M. JONES, *J. Molec. Struct.* **5**, 1 (1970).
[31] A. M. DWIVEDI and S. KRIMM, *Macromolecules* **15**, 177 (1982).
[32] E. W. SMALL, B. FANCONI and W. L. PETICOLAS, *J. chem. Phys.* **52**, 4369 (1970).
[33] M. BEER, H. B. KESSLER and G. B. B. M. SUTHERLAND, *J. chem. Phys.* **29**, 1097 (1958).
[34] J. L. WOOD, in *Spectroscopy and Structure of Molecular Complexes* (edited by J. YARWOOD). Plenum, New York (1973).
[35] S. BRATOS, J. LASCOMBE and A. NOVAK, in *Molecular Interactions*, Vol. 1 (edited by H. RATAJCZAK and W. J. ORVILLE-THOMAS). John Wiley, New York (1980).
[36] Y. MARECHAL, in *Molecular Interactions*, Vol. 1 (edited by H. RATAJCZAK and W. J. ORVILLE-THOMAS). John Wiley, New York (1980).
[37] A. WITKOWSKI and M. WOJCIK, *Chem. Phys.* **21**, 385 (1977).
[38] H. BOUTIN and S. YIP, *Molecular Spectroscopy with Neutrons*, p. 202. MIT Press, Cambridge (1968).